Quaternary Science Reviews 112 (2015) 1–16

Contents lists available at ScienceDirect

Quaternary Science Reviews

journal homepage: www.elsevier.com/locate/quascirev

Invited review

The relative importance of methane sources and sinks over the Last Interglacial period and into the last glaciation

A. Quiquet [a, *], A.T. Archibald [a, b], A.D. Friend [c], J. Chappellaz [d, e], J.G. Levine [f], E.J. Stone [g], P.J. Telford [a, b], J.A. Pyle [a, b]

[a] University of Cambridge, Department of Chemistry, Cambridge, UK
[b] National Centre for Atmospheric Science, UK
[c] University of Cambridge, Department of Geography, Cambridge, UK
[d] Univ. Grenoble Alpes, LGGE, F-38000, Grenoble, France
[e] CNRS, LGGE, F-38000, Grenoble, France
[f] University of Birmingham, School of Geography, Earth and Environmental Sciences, Birmingham, UK
[g] University of Bristol, School of Geographical Sciences, Bristol, UK

ARTICLE INFO

Article history:
Received 26 June 2014
Received in revised form
7 January 2015
Accepted 8 January 2015
Available online

Keywords:
Quaternary
Methane
Chemistry–climate interactions
Land surface emissions
Last Interglacial
Numerical models

ABSTRACT

All recent climatic projections for the next century suggest that we are heading towards a warmer climate than today (Intergovernmental Panel on Climate Change; Fifth Assessment Report), driven by increasing atmospheric burdens of anthropogenic greenhouse gases. In particular, the volume mixing ratio of methane, the second-most important anthropogenic greenhouse gas, has increased by a factor of ~2.5 from the beginning of the European Industrial Revolution. Due to their complex responses to climatic factors, understanding of the dynamics of future global methane emissions and sinks is crucial for the next generation of climate projections. Of relevance to this problem, the Earth likely experienced warmer average temperatures than today during the Last Interglacial (LIG) period (130–115 kaBP). Interestingly, ice cores do not indicate a different methane mixing ratio from the Pre-Industrial Holocene (PIH), in other words the current interglacial period prior to anthropogenic influence. This is surprising as warmer temperatures might be expected to increase methane emissions. The present study aims to improve our understanding of the changes in the global methane budget through quantifying the relative importance of sources and sinks of methane during the last full glacial–interglacial cycle.

A fairly limited number of studies have investigated this cycle at the millenium time scale with most of them examining the doubling in CH_4 from the Last Glacial Maximum (LGM) to the PIH. Though it is still a matter of debate, a general consensus suggests a predominant role to the change in methane emissions from wetlands and only a limited change in the oxidising capacity of the atmosphere. In the present study we provide an estimate of the relative importance of sources and sinks during the LIG period, using a complex climate–chemistry model to quantify the sinks, and a methane emissions model included in a global land surface model, for the sources. We are not aware of any previous studies that have explicitly tackled sources and sinks of methane in the previous interglacial. Our results suggest that both emissions and sinks of methane were higher during the LIG period, relative to the PIH, resulting in similar atmospheric concentrations of methane. Our simulated change in methane lifetime is primarily driven by climate (i.e. air temperature and humidity). However, a significant part of the reduced methane lifetime is also attributable to the impact of changes in NO_x emissions from lightning. An increase in biogenic emissions of non-methane volatile organic compounds during the LIG seems unlikely to have compensated for the impact of temperature and humidity. Surface methane emissions from wetlands were higher in northern latitudes due to an increase of summer temperature, whilst the change in the tropics is less certain. Simulated methane emissions are strongly sensitive to the atmospheric forcing, with most of this sensitivity related to changes in wetland extent.

* Corresponding author.
E-mail address: aurelien.quiquet@gmail.com (A. Quiquet).

http://dx.doi.org/10.1016/j.quascirev.2015.01.004
0277-3791/

1. Introduction

Methane is the second most important anthropogenic greenhouse gas (GHG) after CO_2, accounting for approximately one third of the radiative forcing of CO_2. Around the 1980s, the observed growth rate of methane was as high as 16 ppbv (parts per billion by volume) per year, equivalent to a ~1% increase every year. This growth was sustained until the mid 1990's and after a subsequent decade of near stability, atmospheric methane mixing ratio started to rise again in 2005. The atmospheric mixing ratio of methane is the result of the balance between sources and sinks. Natural sources are very diverse and present three different origins: biogenic (such as wetlands, fresh waters, ruminants, termites), thermogenic (such as natural gas) and pyrogenic (wildfires). Some sources are a mix of different origins, like hydrates, which have both a biogenic and/or thermogenic origin. However, wetlands dominate these natural emissions, representing around 60–80% of the total (Intergovernmental Panel on Climate Change Fifth Assessment Report, Chapter 6, Table 6.8). Methane is produced in soils by methanogenic archeae. The amount and quality of organic substrate, temperature, and oxic level are the main drivers for methanogenesis (Bridgham et al., 2013, and references therein). The methane produced, mostly in anoxic soil layers, can be oxidised in the upper oxic layers. Vegetation can also play a role in the transport and oxidation of methane. Methane emissions are therefore strongly ecosystem-dependant and a large spatial and temporal variability is observed (Jackowicz-Korczyński et al., 2010; Turetsky et al., 2014). Some processes related to methane production are still poorly understood (e.g. microbial community dynamics and the roles of vascular plants), and even the present day global emission rate is still largely uncertain (Kirschke et al., 2013). However, despite the complexity of the interplay of different factors, methane emissions do display a consistent response to temperature across ecosystems (Yvon-Durocher et al., 2014).

After a certain time (broadly defined the lifetime, τ), a fraction of the emitted methane is either oxidised in the troposphere or stratosphere, or oxidised at the surface. The lifetimes we discuss here can be calculated as the reciprocal of the observed (or calculated) rates of loss of the compounds and are termed e-folding lifetimes. The major oxidising species for many hydrogen bearing compounds is the hydroxyl radical (OH). OH is very short lived ($\tau < 0.5$ s). OH is formed as a break down product from the photolysis of O_3 and subsequent reaction with H_2O. Given that the rate of photolysis of O_3 depends strongly on the abundance of O_3, and that the amount of water in the atmosphere can be strongly modified by temperature, there are many complexities and nuances that need to be included in models if they are to represent the oxidation of compounds by OH correctly. Indeed, in the recent Atmospheric Chemistry–Climate Modelling Intercomparison (ACCMIP) tropospheric OH was evaluated for the present day and changes from the PIH to the present, and for changes out to the year 2100 under a range of future emission and climate scenarios (Naik et al., 2013; Voulgarakis et al., 2013). The inclusion of photolysis algorithms that take into account the interactive changes in trace gases and aerosols is something that has only recently become common place within the 3D chemistry modelling community and even within ACCMIP several models used precalculated photolysis frequencies and assumed they would be valid under changes in composition. The reaction between OH and CH_4 in the troposphere accounts for about 85% of CH_4 removal. Stratospheric OH and tropospheric chlorine oxidation, together with soil oxidation, explain the remaining sinks. Owing to the complications with modelling OH, and the fact that the rate coefficient for the reaction between OH and CH_4 is one of the most strongly temperature sensitive reactions that occurs in the atmosphere, modelling methane oxidation accurately is a major challenge. Because tropospheric methane oxidation represents a significant loss for tropospheric OH, methane produces a positive feedback on the climate system, as its lifetime increases with its mixing ratio (e.g. Prather, 2007). Also, methane is a precursor of tropospheric ozone and stratospheric water vapour, which are both GHGs. A breakdown of source and sink strengths in the recent past is presented in Table 1.

Both the sources and the sinks of methane are strongly climate-dependant. With respect to the sources, changes in hydrological regime can affect the global wetland extent (e.g. Bousquet et al., 2006), whilst temperature is the main driver for methane emissions from these wetlands (e.g. Christensen et al., 2003; Turetsky et al., 2014). Whilst with respect to the sinks, the rate of methane oxidation by hydroxyl radicals increases with temperature. In addition to this direct effect, several indirect effects take place, including the increase in OH concentration due to an increase in humidity and the temperature dependency of non-methane volatile organic compound (NMVOC) emissions. However, even for the recent past the interplay of these different components of the methane budget is still a great matter of debate (Kirschke et al., 2013). The investigation of past changes can inform our understanding of natural variations in the budget and the role of changing climate. In particular, air of past atmospheres has been trapped in bubbles in ice cores. Such a direct record of past atmospheric composition is available for the last 800,000 years (Loulergue et al., 2008). Methane and CO_2 are usually stable in ice cores and the records they yield overlap with recent direct atmospheric measurements (e.g. MacFarling Meure et al., 2006), such as those made at Mauna Loa (Keeling et al., 1976).

As illustrated in Fig. 1, on the glacial–interglacial time scale, the methane atmospheric mixing ratio ranges from ~320 ppbv during cold glacials to ~780 ppbv during warm interglacials (Loulergue et al., 2008). However, the ice-core records show that great variations can also occur on shorter time scales. For example, the rise in temperature at the beginning of Dansgaard–Oeschger (DO) events

Table 1
Sources and sinks of methane from natural origin (excluding anthropogenic contribution) over three decades (adapted from Table 1 of Kirschke et al., 2013). The estimates are listed separately for top-down (inverse methods) and bottom-up (process-based). The uncertainty range is provided in brackets. See the original publication of Kirschke et al. (2013) for the complete list of references.

	1980–1989		1990–1999		2000–2009	
	Top-down	Bottom-up	Top-down	Bottom-up	Top-down	Bottom-up
Sources						
Wetland	167 [115–231]	225 [183–266]	150 [144–160]	206 [169–265]	175 [142–208]	217 [177–284]
Non-wetland	36 [35–36]	130 [61–200]	32 [23–37]	130 [61–200]	43 [37–65]	130 [61–200]
Total sources	**203 [150–267]**	**355 [244–466]**	**182 [167–197]**	**336 [230–465]**	**218 [179–273]**	**347 [238–484]**
Sinks						
Chemical loss	490 [450–533]	539 [411–671]	525 [491–554]	571 [521–621]	518 [510–538]	604 [483–738]
From which tropospheric OH		*468 [382–567]*		*479 [457–501]*		*528 [454–617]*
Soils	21 [10–27]	28 [9–47]	27 [27–27]	28 [9–47]	32 [26–42]	28 [9–47]
Total sinks	**511 [460–559]**	**539 [420–718]**	**542 [518–579]**	**596 [530–668]**	**540 [514–560]**	**632 [592–785]**

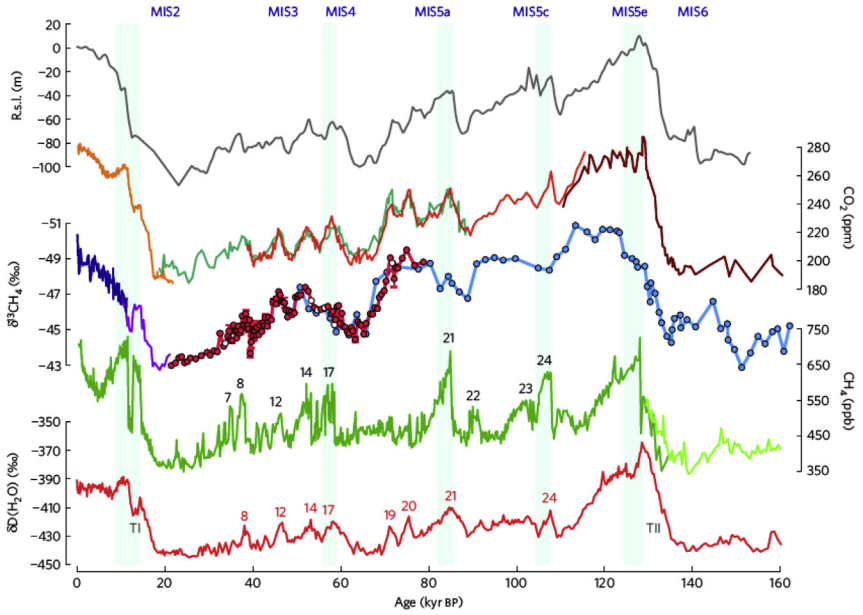

Fig. 1. Methane carbon isotope and other climate records. From top: relative sea-level (r.s.l.) reconstruction. Atmospheric CO_2 from Vostok (brown), EDML and Talos Dome (orange), Byrd (turquoise) and EPICA Dome C (yellow), in parts per million (ppm). $\delta^{13}CH_4$ from Vostok (light blue) and EDML (dark red). Records for termination 1 (TI; EDML, purple) and the Holocene (Greenland Ice Sheet Project Two (GISP2), dark blue). Samples potentially affected by diffusive fractionation are marked by white circle fillings. Atmospheric CH_4 from EDC (light green) and EDML (dark green). δD in precipitation at Dome C (red). Arabic numbers indicate the timing of Dansgaard–Oeschger events and their respective Antarctic counterparts. Vertical bars indicate periods when the correlation between CO_2 and CH_4 breaks down. TII, termination 2. Reprinted by permission from Macmillan Publishers Ltd: Nature Geoscience (Möller et al., 2013), copyright 2013.

are, most of the time, accompanied by an increase in methane over a century (Landais et al., 2004; Baumgartner et al., 2014; Rosen et al., 2014). A better investigation of such rapid changes in the global methane budget has been possible very recently thanks to the improvements in measuring techniques, which showed that the rate of methane increase could have reached 2.5 ppbv/yr at the beginning of DO events (Chappellaz et al., 2013; Rosen et al., 2014). Ice core records originating from the two major ice sheets (i.e. Antarctica and Greenland) provide coarse information of the latitudinal variations in the balance between methane sources and sinks, via the interpolar gradient in methane mixing ratio. This gradient has been mostly used to infer latitudinal shifts in methane sources during the Holocene and during DO events (Chappellaz et al., 1997; Dällenbach et al., 2000; Baumgartner et al., 2012).

In this paper, we review current knowledge of global methane dynamics during the Last Glacial–Interglacial cycle, that is changes in sources and sinks. In particular, we discuss the glacial–interglacial amplitude, the so-called Holocene anomaly, and the rapid rise in methane at the onset of Dansgaard–Oeschger events. Finally, we present a recent contribution to this topic in a relatively unexplored period, the Last Interglacial (LIG) (130–115 kaBP). This period of time presents a unique opportunity to study the methane global cycle in a warmer than today climate but with a similar geography. It is also something of a curiosity that, though the climate was warmer than in the PIH, the volume mixing ratio of methane in the atmosphere was no higher; this represents a departure from the first-order observation from the ice core records that methane mixing ratios generally increase (decrease) as the climate warms (cools).

2. An overview of global methane over the Last Glacial–Interglacial cycle

2.1. Measuring past fluctuations in methane

The first major studies which intended to quantify the methane budget in the past were motivated by the availability of a comprehensive record of past fluctuations in deep ice core drillings. However, before the first military (Camp Century) and non-military (Dye 3) deep ice core drilling programs, scientists examined the air trapped in ice bubbles from different ice samples in ice sheets. For example, Robbins et al. (1973) gave estimates of past changes of both carbon monoxide and methane from a selection of different ice samples of Greenland and Antarctica. Following a similar experimental methodology, Khalil and Rasmussen (1985) extrapolated potential human activities to the past in order to quantify the importance of sources and sinks of methane.

Deep ice core records have resulted in a hugely significant amount of information regarding GHG concentrations in the past. The first long methane record (several thousand years) was derived from measurements in Greenland (Craig and Chou, 1982), followed by measurements in Antarctica (Raynaud et al., 1988; Stauffer et al., 1988), where the very low accumulation rate allows the record to go further back in time. At the beginning of the 1990s, the first record covering the Last Glacial–Interglacial cycle was available (Chappellaz et al., 1990). This methane record from the Vostok ice core drilled in Antarctica eventually reached back 420,000 years on a continuous time scale (Petit et al., 1999). A new record went even further back in time to 800,000 years with the drilling of EPICA-DOMEC ice core (Spahni et al., 2005; Loulergue et al., 2008). Unfortunately, in Greenland the signal during the Last Interglacial period is perturbed in all the six deep ice cores due to layer mixing, past surface melting or basal melting. This is also the case in the latest one to be drilled (NEEM Members, 2013). Nevertheless, suitable Greenland methane records covering the last 100,000 years have allowed researchers to evaluate the interpolar gradient and its possible evolution through time (e.g. Baumgartner et al., 2012). Available comparisons between Greenland and Antarctic mixing ratios during cold stadial to warm interstadial transitions during the Last Glacial period (e.g. the onset of DO events) suggest a northward shift of the methane sources associated with each interstadial warming event.

Methane mixing ratio and its interpolar gradient are not the only information available about past fluctuations. Two of the minor stable isotopologues of methane, namely those in which carbon thirteen ($^{13}CH_4$) or deuterium atom ($^{2}H(CH_4)$ or $D(CH_4)$) are substituted for the common isotopes ^{12}C and H, are also preserved in ice cores (Fig. 1). The isotopic signature is defined as the ratio between the heavier and lighter stable isotopologues compared to a reference value and is denoted $\delta^{13}CH_4$ for carbon thirteen and $\delta D(CH_4)$ for deuterium. Methane carbon stable isotopic signatures are associated with different sources. The processes that control the formation of methane set the value of the isotope ratios. These can range from methane very depleted in ^{13}C, the heavy isotopologue, from microbial origin like some gas hydrates and wetlands (~−70 to ~−60‰) to heavier CH_4 associated with biomass burning (~−25‰). Atmospheric oxidation contributes to a relatively small fractionation (ε_C), enriching the atmosphere in ^{13}C compared to the average of methane sources by about ~7.4‰ (Whiticar and Schaefer, 2007). However, changes in the relative strengths of different methane sinks, in particular the relative strength of the atomic chlorine sink, can affect this number, for example in response to glacial–interglacial changes in atmospheric circulation (Levine et al., 2011a). It is therefore not entirely correct – it is an approximation – to treat $\delta^{13}CH_4$ simply as an indicator of changes in methane sources (Möller et al., 2013). Hydrogen stable isotopes are more difficult to use as the atmospheric fractionation (ε_D) is much greater, being around 200‰ (Whiticar and Schaefer, 2007). However, $\delta D(CH_4)$ can be used to distinguish hydrate sources, as it shows a large difference compared to other sources. Also, during methane production at the Earth's surface, the radioactive isotope ^{14}C is also included in the molecule (via atmospheric CO_2 assimilation by photosynthesis), but in a much smaller proportion than ^{13}C and ^{12}C due to its rarity. Due to the long time periods involved, ^{14}C is virtually absent from geological sources of methane. Therefore the proportion of ^{14}C in the atmospheric methane reservoir is an indicator of the relative proportion between geological and modern biogenic sources (Wahlen et al., 1989). Although an experimental challenge, pioneering measurements of $^{14}CH_4$ carried out on glacial outcrops of the Greenland ice sheet covering the last deglaciation showed that methane hydrate degassing was not responsible for the rapid CH_4 jumps punctuating this major climatic transition (Petrenko et al., 2009; Melton et al., 2012).

2.2. On the amplitude of glacial – interglacial methane concentrations

One striking feature observed from the methane measurements in ice cores is the strong contrast between the low Last Glacial Maximum (LGM) methane level of ~350 ppbv and the Pre-Industrial Holocene (PIH) value of ~700 ppbv (Fig. 1). Explaining the potential causes of this doubling is still one of the main challenges in palaeo-methane science. Motivated by the results of the Vostok drilling project, Raynaud et al. (1988) and Chappellaz et al. (1990) provided the first hypothesis for the changes in source reduction during the LGM, whilst McElroy (1989) and Valentin (1990) studied glacial–interglacial changes in oxidative capacity. However, Chappellaz et al. (1993) and its companion paper Thompson et al. (1993), were the first comprehensive studies of all the different components of the global budget and their relative changes at the LGM. In Chappellaz et al. (1993), vegetation and wetland reconstructions suggested a 44% reduction in the wetland source during the LGM. In addition to the presence of extensive ice sheets, a cold and dry climate may have reduced wetland extent and therefore methane emissions. The reduction in the sources they reconstructed was fed into a multi-box one-dimensional model of atmospheric chemistry in Thompson et al. (1993). They were able to achieve an agreement between their bottom-up model estimates and ice core derived methane mixing ratio. They concluded that the glacial–interglacial methane change was mostly a source-driven signal. Using a very similar atmospheric chemistry box model, Pinto and Khalil (1991) and Lu and Khalil (1991) suggested an almost stable hydroxyl radical concentration between the LGM and the PIH, again implying an almost entirely source-driven change in methane mixing ratio. They suggest that during cold glacials, the decreased loss of OH (due to lower methane) is compensated by a lower production (due to lower humidity). This was later corroborated by Karol et al. (1995) who used a multi-box (troposphere and stratosphere), one dimensional model. The complexity of atmospheric chemistry representation increased with the work of Crutzen and Brühl (1993), who used for the first time a 1½D model (vertically resolved with two hemispheres) chemistry–radiation model, including a representation of the stratosphere. Here again, even if the different components of OH budget differed under glacial conditions, changes in the OH mixing ratio were very small. This was subsequently reproduced with an even more sophisticated 2D chemistry–radiation model by Martinerie et al. (1995), who estimated an increase by 20% of the global mean OH concentration during the LGM compared with PIH values. Thus, the early studies suggested that the change in methane mixing ratio from LGM to PIH was mostly source driven.

However, the question of the relative importance of sources and sinks over this time period was revisited in the work of Kaplan (2002). For the first time, a process-based model of methane emissions from wetlands was used to provide estimates of the source changes. In this study the low levels of CO_2 during the LGM led to a reduction in vegetation productivity and, as a consequence, of the substrate availability for methanogenesis. However, the changes in methane emissions from wetlands could not explain the total glacial–interglacial change in methane mixing ratio, implying a change in oxidising capacity was required to explain the remainder. Weber et al. (2010) followed the same methodology of Kaplan (2002) but for a set of eight climatic forcings from the Paleoclimate Modelling Intercomparison Project (PMIP2). In this study, they tested the sensitivity of a process-based model of methane emissions to atmospheric forcing. Weber et al. (2010) modelled a range of reductions in methane emissions from wetlands at the LGM that were greater than the reduction calculated by Kaplan (2002). The largest of these reductions, combined with changes in other methane sources besides wetlands, would be sufficient to account for the entire change in methane concentration at the LGM without recourse to a significant change in oxidising capacity; see later. However, smaller reductions would still imply the need for an increase in oxidising capacity. Valdes et al. (2005) subsequently suggested that the reduction in NMVOC emissions from vegetation at the LGM, relative to the PIH, could explain at least some of the mismatch. Valdes et al. (2005) tested this hypothesis in an Earth System Model (ESM) framework, including a 3D atmospheric chemistry model, and concluded that in order to achieve an agreement with ice core measurements, changes in both methane sources and sinks were needed. Kaplan et al. (2006) reached the same conclusions in a further model framework. Note, however, that Kaplan et al. (2006) explored only the impact of reduced NMVOC emissions from vegetation; they did not explore the opposing influences of reduced humidities at the LGM, reducing the availability of OH, and reduced air temperatures at the LGM, reducing the rate of reaction between OH and methane. Harder et al. (2007) carried out a series of sensitivity experiments with a chemistry–climate model, highlighting the sensitivity that the lifetime of methane shows to reductions in air temperatures and humidities. Using a global atmospheric Chemistry Transport Model (CTM), Levine et al. (2011b) found these influences to almost

precisely negate the reduction in methane lifetime due to reduced NMVOC emissions at the LGM, resulting in a negligible net change in methane lifetime. The implication was that the glacial–interglacial change in methane mixing ratio must have been almost entirely source-driven – the suggestion of the early studies. The mutually compensating influences on the oxidising capacity reported by Levine et al. (2011b) have since been reproduced by Murray et al. (2014) using a state-of-the-art 3D chemistry–climate model including tropospheric- and stratospheric chemistry, and for the first time, interactive photolysis. Murray et al. (2014) additionally reported that the oxidising capacity they modelled was insensitive to changes in biomass burning emissions (reactive species and aerosol precursors), but sensitive to changes in lightning-induced NO_x emissions – in line with the earlier findings of Murray et al. (2013).

In summary (see also Table 2 for a compilation), most of the recent chemistry–climate studies to date tend to suggest a constant or only slightly decreased methane lifetime at the LGM. An exception is the top-down study by Fischer et al. (2008) that explores, by a Monte-Carlo approach, possible methane source- and sink-change scenarios compatible with the observed changes in methane concentration and isotopic composition. They suggest that the lifetime of methane was likely significantly reduced at the LGM, but offer no process-based explanation. They also propose that boreal wetland sources of methane were effectively shut down at the LGM, whilst emissions of methane from biomass burning were largely unchanged relative to the PIH. However, the reanalysis by Baumgartner et al. (2012) of the inter-polar gradient in methane concentration at the LGM suggests that, whilst boreal wetland sources (above 30°N) were reduced, they were not shut down, and the global synthesis of charcoal records by Power et al. (2008) suggests there was markedly less biomass burning at the LGM. As for bottom-up estimates of the changes in methane emissions at the LGM, the most recent estimates regarding methane emissions from wetlands, by Weber et al. (2010), range from a reduction of 35% to one of 42% relative to the PIH. Combined with the estimates of Valdes et al. (2005) and Kaplan et al. (2006) of the changes in methane emissions from other sources besides wetlands, reductions in total methane emissions of 30–35% and 38–43% are obtained respectively. Though it may be one extreme, Levine et al. (2011b) note that, allowing for the small positive feedback between changes in methane concentration and lifetime (Prather, 2007), a 43% reduction in total methane emissions could account for almost the entire 49% reduction in methane concentration observed (from 700 to 360 ppbv) without invoking any further reduction in methane lifetime. Increased confidence in our understanding of the methane budget at the LGM should be sought through further comprehensive chemistry–climate studies and methane source-change estimates.

Table 2
Relative change of OH and methane surface emissions during the LGM compared to PIH in the literature. Note that the change in methane lifetime also includes the effect of temperature on the reaction rate and is not only the consequence of the change in OH.

Study	Chemistry model	LGM vs. PIH changes	
		[OH]	$\tau_{CH_4,OH}$ (if provided)
Valentin (1990)	2D	+23%	–
Pinto and Khalil (1991)	1D	+15%	–
Lu and Khalil (1991)	1D	+26%	–
Crutzen and Brühl (1993)	Multi-box 1D	+10%	–
Thompson et al. (1993)	Multi-box 1D	+10%	–
Martinerie et al. (1995)	2D	+20%	−17%
Karol et al. (1995)	Multi-box 1D	−59% to +14%[a]	–
Valdes et al. (2005)	3D	+25%[a]	−15%
Kaplan et al. (2006)	3D	+28%	−22%
Levine et al. (2011b)	3D	–	+2%
Bock et al. (2012).	2D	+14%	−11%
Murray et al. (2014)	3D	+2%	−2% to +35%

Study	Surface emissions	LGM vs. PIH changes	
		Wetland emissions	All sources (if provided)
Chappellaz et al. (1993)	Vegetation and wetland reconstruction	−44%	–
Kaplan (2002)	Process-based wetland model	−24%	–
Valdes et al. (2005)	Process-based wetland model	−27%	−23%
Kaplan et al. (2006)	Process-based wetland model	−21%	−16%
Weber et al. (2010)	Process-based wetland model	−42% to −35%	–

[a] The reported change in OH for those studies is a change in the surface mean concentration and not tropospheric mean.

2.3. On the Dansgaard–Oeschger events

Other intriguing features of the methane record are the very sharp rises in methane (~100 ppbv within a century) at the onset of Dansgaard–Oeschger (DO) events. This topic has been addressed recently by Levine et al. (2012), who suggested that temperature impacts on oxidation rates (via reaction rate and humidity) and NMVOC emission changes have a compensating effect, leading to an almost stable oxidising capacity between cold stadials and warm interstadials. Though they find that the combined influence of changes in temperature and humidity slightly outweighs the influence of changes in NMVOC emissions, this is qualitatively a very similar finding to that of (Levine et al., 2011b) regarding the mutually compensating influences on the oxidising capacity between the LGM and the PIH. Interestingly, Ringeval et al. (2013), using two different process-based models of natural methane emissions from wetlands during idealised DO events, were only able to simulate 25% of the ice core measured range. With a fully coupled model, Hopcroft et al. (2011, 2014) drew the same conclusions, and emphasised the apparent insensitivity of current models to surface emissions. However, likewise most of process-based approaches, Ringeval et al. (2013) and Hopcroft et al. (2011, 2014) only consider changes in the wetland contribution and do not investigate other contributors. Also, part of the inability of reproducing the magnitudes of changes using bottom-up approaches may come from an over-simplified representation of the different processes (Zürcher et al., 2013). In particular, a better representation of peatlands has been developed and analysed (Kleinen et al., 2012; Schuldt et al., 2013). Destabilisation of clathrates has also been proposed as an explanation for the rapid rise in methane during DO events or during the Bölling–Allerod (e.g. Nisbet, 1992; Kennett et al., 2003; Nisbet and Chappellaz, 2009). For this reason, clathrate models have been recently implemented in some bottom-up estimates of methane emissions (Reagan and Moridis, 2007; Archer et al., 2009). However, analysis of the isotopic composition of methane does not suggest any major clathrate degassing event during the Last Glacial nor deglacial periods (Brook et al., 2000; Schaefer et al., 2006; Sowers, 2006; Petrenko et al., 2009; Bock et al., 2010; Melton et al., 2012). The review of Maslin et al. (2010) evaluated the past and future potential impacts of this process, but stated that a definitive answer on this topic is not yet possible given that the carbon stock still lacks evaluation, and that our knowledge on the destabilisation processes still needs improvement.

Broadly speaking, the results of investigations of the DO events overlap with the results of the LGM to PIH changes in methane. In both cases, atmospheric chemistry studies tend to suggest a fairly limited net impact on sink changes on the methane lifetime (due to significant but compensating individual influences), and are

consistent with isotopic signature changes recorded in ice cores. At the same time, bottom-up estimates from natural wetlands apparently tend to underestimate the amplitude of the changes. However, these findings rely on a very few studies and therefore, as for the LGM, further assessments with process-based models of sources and sinks are still needed in order to be confident in their potential changes.

2.4. On the Holocene "anomaly"

The rises of the methane mixing ratio through the last termination (end of the glacial period) and at the onset of the DO events are not the only striking features of methane dynamics observed in the ice cores. Unexpectedly, after a typical decrease in the early Holocene following the insolation trend, the methane concentration started to rise again 5000 years ago (Blunier et al., 1995). This pattern was not observed during the LIG: the decreasing insolation and its impact on the monsoon (Kutzbach, 1981) led to decreasing methane levels, and is followed by glacial inception. This Holocene "anomaly" has led Ruddiman (2003) to suggest that early human activities (essentially early agriculture and forest clearance) significantly perturbed the global carbon cycle, an explanation already suggested by Chappellaz et al. (1997) to explain the observed interpolar gradient decrease during the second half of the Holocene. The possibility that the human population, very reduced at the time, could have such an effect on atmospheric composition is highly controversial. However, the long-term trend in isotopic signature of methane seems to be consistent with early land use change (Mischler et al., 2009; Sapart et al., 2012). Also, insolation-modulated monsoon and archaeological reconstructions of early rice paddies in China appear to support this scenario (Zhou, 2012). However, Burns (2011) suggested that the hydrological changes in the inter-tropic region recorded in speleothems could be sufficient to explain the characteristics of the atmospheric methane concentrations during the Holocene. Very few modelling studies of such a subject exist, and they tend to disagree. In a comprehensive model framework including NMVOC and methane emissions, Singarayer et al. (2011) suggested that an orbitally driven change in tropical sources can explain the Holocene anomaly, without invoking any early land use change. However, using a similar model framework but a less sophisticated model, Konijnendijk et al. (2011) were unable to reach the same conclusions. The reason for the rise in methane during the late PIH could be a mixed consequence of natural and anthropogenic contributions. Thus, Mitchell et al. (2013) investigated the interpolar gradient evolution over this period. Their analysis suggests that even if the major part of the signal is a tropical wetland response to changing insolation, an anthropogenic contribution is needed to account for the rise in emissions at mid-latitudes. Unfortunately, no study has yet fully investigated the potential consequences of atmospheric chemistry changes over this period. Singarayer et al. (2011), for example, explored the influence of changes in NMVOC emissions, but did not explore the opposing influences of changes in air temperature and humidity. Therefore, future work should look into the impact of insolation changes on methane oxidation.

3. Modelling the last interglacial sinks and sources

In this section, we focus on the LIG period because of its apparent anomaly: the global climate was likely warmer, especially at high latitudes (Anderson et al., 2006), but the methane mixing ratio was very similar to the PIH levels (Loulergue et al., 2008). This period has not been investigated to date with comprehensive process-based models and so such analysis could give us important insights into methane source and sink responses to orbital forcing changes in a warmer climate than present.

3.1. The change in the LIG atmospheric methane sinks

We use the UKCA chemistry–climate model (Morgenstern et al., 2009; O'Connor et al., 2014) to investigate the changes in atmospheric sinks of methane during the LIG. We use the atmosphere only set-up described in Banerjee et al. (2014) with a horizontal resolution of $2.5^\circ \times 3.75^\circ$ and 60 vertical layers from the surface to 84 km. Sea surface temperature (SST) and sea ice concentrations are specified. The chemistry simulates the O_x, HO_x and NO_x chemical cycles and the oxidation of CO, ethane, propane and isoprene (O'Connor et al., 2014) as well as chlorine and bromine chemistry (Morgenstern et al., 2009). Nine species are emitted (NO, CO, HCHO, C_2H_6, C_3H_8, $(CH_3)_2CO$, CH_3CHO, C_5H_8 and CH_3OH), with a further six species (N_2O, CF_2Cl_2, $CFCl_3$, CH_3Br, H_2, and CH_4) prescribed, at the surface. Although methane, and these other gases, are constrained at the surface, they are freely able to evolve in the atmosphere (troposphere and stratosphere). Photolysis rates are interactively computed with FAST-JX (Telford et al., 2013) for each reaction and over 18 wavelength bins. A thorough calculation of the optical depth (from water clouds, aerosols, oxygen, ozone and Rayleigh scattering) is performed to evaluate scattering. Thus, photolysis rates change between simulations.

For our control simulation (pre-industrial, hereafter PIH), we run a 30-year timeslice experiment. SST and sea ice fraction, were taken from HadISST dataset (Rayner et al., 2003) as in Archibald et al. (2011). Surface emissions are those of Lamarque et al. (2010) for the year 1850 and those of Guenther et al. (2006) for natural emissions. Based on our control PIH run, we also constructed an idealised Last Interglacial (LIG) in which the only changing conditions from the control are the oceanic boundary conditions (sea surface temperature and sea ice fractions) and the orbital forcings. The oceanic fields were extracted from Lunt et al. (2013a) (HadCM3, 125 kaBP snapshot). Lunt et al. (2013a) use an earlier version of the unified model, with no chemistry, but with a dynamic ocean. The orbital forcings (namely eccentricity, obliquity and precession) were chosen to be the same as in Lunt et al. (2013a) for the 125 kaBP conditions. As stated in the introduction, during the LIG and the PIH periods, the mixing ratio of the GHGs (such as CO_2, N_2O and CH_4) were similar (e.g. Wolff and Spahni, 2007). Hence, no changes were made to trace gas emissions from the PIH for the idealised LIG. Biomass burning changes for the LIG are difficult to assess. There are a number of charcoal records covering the last deglaciation, but very few reach back the LIG (Power et al., 2010). However, there is some evidence suggesting limited changes (possibly decreases) in biomass burning during the LIG compared to the PIH (e.g. Zhou et al., 2007; Lawson et al., 2013). Because the changes in biomass burning are uncertain, and likely small, we do not attempt to simulate them. In addition, Murray et al. (2014) have tested a range of biomass burning scenarios for the LGM and PIH and they have

Table 3
Boundary conditions of the different chemistry–climate simulations and associated methane lifetime.

Experiment name	Surface emissions	Lightning NO_x	Ocean	Orbital forcing	$\tau_{CH_4,OH}$ (yr)
PIH	PIH	Interactive	PIH	PIH	**9.3**
LIG	PIH	Interactive	LIG	LIG	**8.0**
LIG_{iso}	PIH + LIG isoprenes	Interactive	LIG	LIG	**8.2**
PIH_{LNOx}	PIH	Fixed PIH	PIH	PIH	**9.6**
LIG_{LNOX}	PIH	Fixed PIH	LIG	LIG	**8.5**

found little impact of these on the methane lifetime, giving support to our assumption. Our model simulations allow us to quantify the direct impact of a changing climate in the atmosphere on the chemistry. Indirect impacts, such as changes in surface conditions, are neglected here. We summarise experiment names and boundary conditions in Table 3.

We present the simulated global mean temperature difference between the LIG and PIH periods (i.e. *LIG − PIH*) in Fig. 2a. Compared to the PIH, our simulated LIG annual mean global temperature is only slightly warmer (+0.5 °C), but the seasonality is enhanced (Fig. 2b: DJF −0.3 °C; MAM −0.3 °C; JJA +1.5 °C; SON +1.1 °C). Most of the northern land surface exhibits a slight cooling in the annual mean, while the tropics tend to show a slight warming. Fig. 2a also shows the proxy reconstructions of Turney and Jones (2010) for oceanic and terrestrial temperature anomalies. The proxy-model differences over the continents are generally smaller than 2 °C, except in northern Eurasia where there is strong disagreement, the model being substantially colder. There is also a disagreement over the oceans where our model simulation is mainly driven by the SST reconstructions of Lunt et al. (2013a). Part of the model-data disagreement comes from the fact that Turney and Jones (2010) temperatures represent the maximum temperature recorded at different locations during the whole LIG whilst this climatic optimum was not a synchronous signal (Capron et al., 2014). However, our LIG temperatures are within the range of the multi-model assessment of Lunt et al. (2013a).

These changes in temperature translate into changes in specific humidity (presented in Fig. 3). The climate is generally wetter, especially in monsoon-affected regions. This is in agreement with Braconnot et al. (2008) and possibly related to the enhanced sea-land contrast. We also simulate enhanced deep convection, especially in the tropical band.

These changes in climate have large direct impacts on the sinks of methane. The main sink, oxidation by OH is strongly linked to the ozone budget (summarized in Table 4). Ozone production is primarily controlled by the amount of NO_x. The increased convection in our LIG simulation causes an increase of NO_x produced by lightning. Consequently the production rate is increased during the LIG. The resulting ozone is then photolysed to excited oxygen atoms ($O(^1D)$), which react with water vapour to form OH. Increases in water vapour, related to the wetter climate, also act to increase OH. Independently, the increase of NO due to enhanced convection also directly increases the amount of OH, via the reaction with HO_2 (e.g. Murray et al., 2013). The overall increase in OH reaches up to 40% in the tropical upper troposphere region (Fig. 4). Combined with higher temperatures which act to increase the reaction rate with methane, the methane lifetime is simulated to reduce by 14.0% in the LIG relative to the PIH.

As stated above, we use idealised conditions for the LIG, considering that all surface fluxes of trace gases were the same as for the PIH. As we have very little information about past changes of these emissions, this hypothesis is not unreasonable. However, we do know that biogenic emissions are positively correlated with temperature (and negatively with CO_2) (Guenther et al., 2012). Isoprene is the most important NMVOC and changes in its emissions have been shown to affect the lifetime of methane (Archibald et al., 2011). In order to take into account the impact of temperature changes on isoprene emissions, we derive a simplified equation for the emission activity γ_T of Guenther et al. (2006). This factor γ_T accounts for emission changes due to deviations from standard conditions.

Considering small changes in temperature (T):

$$\frac{\gamma_{T,LIG}}{\gamma_{T,PIH}} = 1 + \left(1 - \frac{C_{T2} \times \exp(C_{T2} \times x_{PIH})}{C_{T2} - C_{T1} \times (1 - \exp(C_{T2} \times x_{PIH}))}\right) \times C_{T1} \times \frac{T_{LIG} - T_{PIH}}{0.00831\ T_{PIH}^2} \quad (1)$$

With $C_{T1} = 95$; $C_{T2} = 230$; and $x_{PIH} = (1/312\text{-}1/T_{PIH})/0.00831$.

Fig. 5 presents the global annual mean differences between the LIG and the PIH as a result of this relationship between isoprene emissions and changes in temperature. We estimate an increase of around +20% during the LIG (up to 100 Tg/yr) compared to PIH. Importantly, we do not account for potential changes in soil moisture, vegetation distribution or leaf area index, which could also affect the isoprene emissions (Guenther et al., 2012). We included the temperature-dependent additional amounts of isoprene to our default LIG run (LIG_{iso} simulation). The decrease in methane lifetime, although slightly less pronounced, is still significant (11.8% compared to 14%, see Table 3). Thus, isoprene emissions, whilst having an impact on the methane lifetime, are unlikely to fully compensate for the effects of temperature and humidity changes, as for the LGM (Levine et al., 2011b). Though much more pronounced for the LIG, the dominant influence of change in air temperature and humidity is allied to the findings of Levine et al. (2012) at the onset of DO events.

Methane lifetime is strongly dependant on the amount of NO_x emitted by lightning (Holmes et al., 2013). As stated earlier, we simulate enhanced deep convection during the LIG producing an increase in lightning NO_x of 20%, which corresponds to an extra 1.27 Tg of NO_x emitted each year (Fig. 6). Our representation of lightning NO_x follows a relatively simple distribution of flash frequency (Price and Rind, 1994), computed from the height of

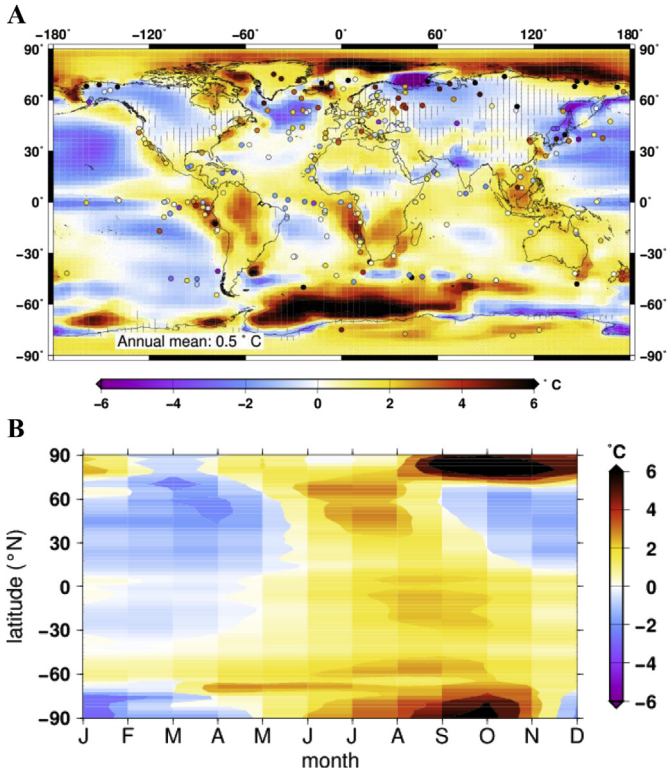

Fig. 2. A: Annual mean surface air temperature anomaly (LIG-PIH). Dots show locations and values of the proxy data from the recompilation of Turney and Jones (2010). Hatched areas represent grid points where a 95% significance level is not reached. B: Zonally averaged monthly-mean surface air temperature anomaly (LIG-PIH).

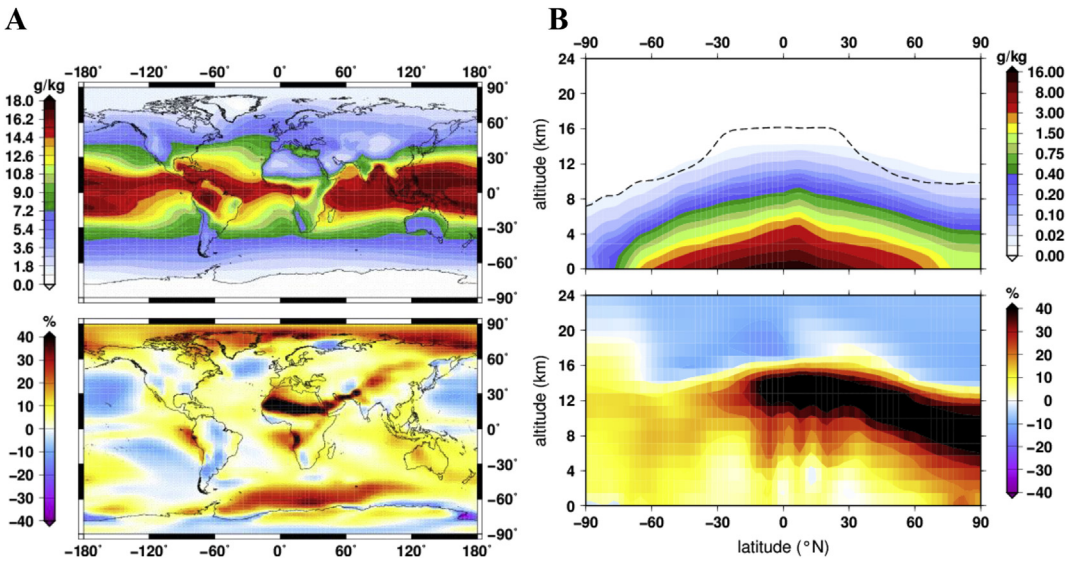

Fig. 3. A: Annual mean surface specific humidity (top) and relative change (*LIG-PIH*, bottom); B: Annual mean zonally averaged specific humidity (top) and relative change (*LIG-PIH*, bottom). The dashed line stands for the altitude of the tropopause diagnosed in the model.

convective clouds. Large uncertainties (e.g. Schumann and Huntrieser, 2007) exist in the simulation of lightning NO_x in global models. Therefore, we test the importance of this process in a sensitivity experiment. In two new experiments, we use the diagnosed climatological monthly lightning NO_x from our control PIH simulation instead of calculating it interactively. Thus, we produced a new PIH simulation with non-interactive NO_x from lightning (PIH_{LNOx}, which differs from the control *PIH* simulation as it does not take into account non-linearity induced by the interactive computation) as well as a new LIG simulation (LIG_{LNOx}). These two simulations have exactly the same amount of NO_x emitted from lightning, reducing the number of differences, though changes in orbit and climate will still yield discrepancies. The change in methane lifetime between these two experiments shows a decrease during the LIG (reduction of 11.5%). Although this decrease is smaller than the standard experiments (*PIH* vs. *LIG*, 14%), it is still significant. This result suggests that NO_x emitted from lightning is a significant driver of methane lifetime, accounting for 18% of the decrease we simulate at the LIG. This process tends to reduce the lifetime of methane in a warmer climate. The importance of lightning has been recently assessed in the projections for future climate of Banerjee et al. (2014). We agree with Banerjee et al. (2014) on the direction of these impacts but it is less pronounced in our simulation, partly because of the relative small changes in NO_x emitted by lightning, and also because of the effects of orbital changes. In our simulations, changes in climate (temperature and humidity) remain the most important factor.

To conclude, we simulate a reduction of methane lifetime during the LIG, due to the change in orbital forcings and their effects on climate. We have tested most of the important factors controlling the methane lifetime: changes in NMVOC emissions, air temperature and humidities (Levine et al., 2011b) and changes in NO_x emitted from lightning (Holmes et al., 2013). We haven't directly tested the impact of potential changes in photolysis rates. However, interestingly, in our simulations the tropical stratospheric ozone remains almost unchanged, leading to a negligible change in the photolysis rates. A ~10% reduction of the methane lifetime during

Table 4
Tropospheric budget of odd oxygen ($Ox = O + O_3 + NO_2 + 2NO_3 + 3N_2O_5 + HNO_4$ + peroxyacyl nitrates) for the different atmospheric simulations. Here we define net Ox as the residual of the gas phase Ox reaction (gas phase Ox production minus gas phase Ox loss). The stratospheric source of ozone in the troposphere is given as the stratosphere–troposphere exchange STE) where we calculate this as a residual term (by including Ox deposition) of the overall Ox budget (see for example Stevenson et al. (2006) for details).

Experiment name	Ox production (10^3 Tg/yr)	Ox losses (10^3 Tg/yr)	Net Ox (Tg/yr)	STE inferred (Tg/yr)	O_3 burden (Tg)	τ_{O_3} (yr)
PIH	3.31	3.17	135.0	553	288	**26.6**
LIG	3.72	3.62	98.0	626	315	**26.1**
LIG_{iso}	3.75	3.70	56.8	675	316	**25.7**
PIH_{LNOx}	3.17	3.07	96.6	570	273	**26.3**
LIG_{LNOX}	3.50	3.42	83.2	612	289	**25.3**

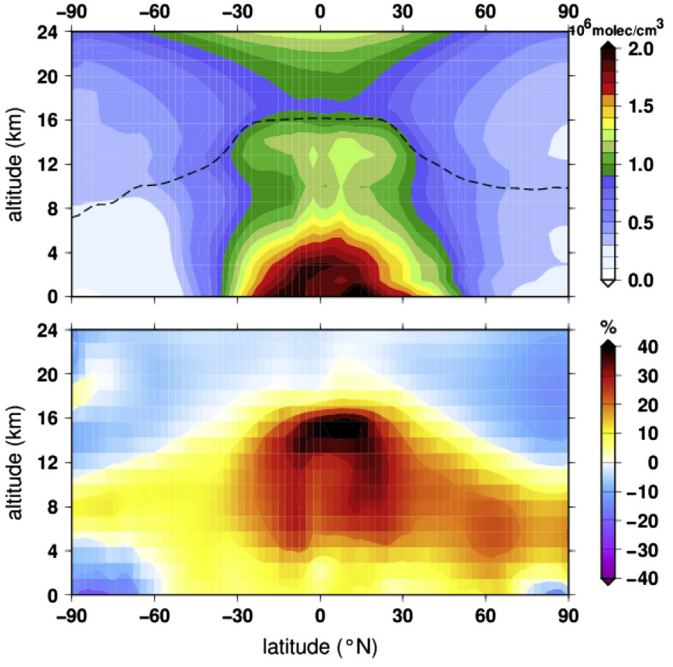

Fig. 4. Annual mean zonally averaged OH mixing ratio (top) and relative change ((*LIG-PIH*)/*PIH*) bottom. The dashed line stands for the altitude of the tropopause diagnosed in the model.

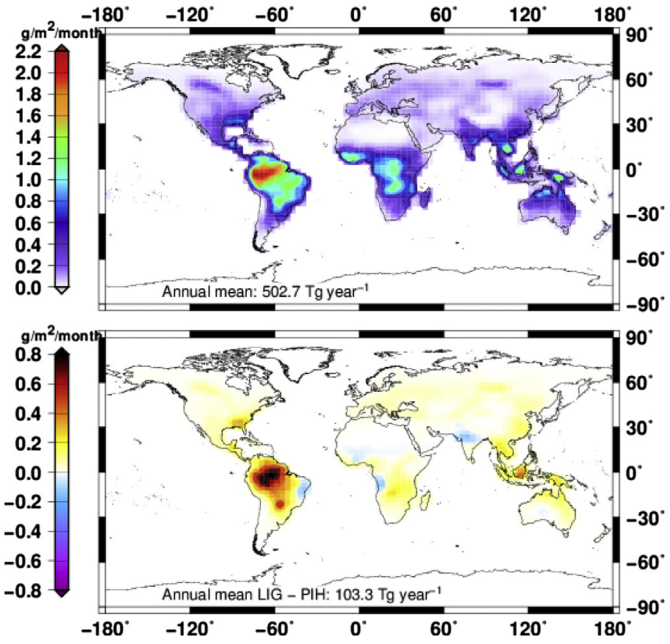

Fig. 5. Annual mean isoprene emissions (top) and differences (*LIG-PIH*) computed with Eq. (3.1) (bottom).

the LIG period appears as a robust finding coming out of our simulations. This implies that to produce a zero net change in the atmospheric mixing ratio from the PIH, roughly a 10% increase in surface methane emissions during the LIG would be expected.

3.2. The change in the LIG methane sources

We have used the Hybrid8 global land surface model to calculate methane emission rates during the LIG. The surface physics of this model are based on the NASA-GISS ModelE land surface component (Schmidt et al., 2006). This model contains a relatively sophisticated canopy representation (Friend and Kiang, 2005), allowing for a realistic simulation of canopy conductance responses to various environmental factors (i.e. light, temperature, humidity, CO_2 and canopy height). The model runs on a $0.5^\circ \times 0.5^\circ$ Cartesian grid and its integrating timestep is 30 min. In this study we generate a daily climatology (Friend, 1998) based on the CRU monthly data (Harris et al., 2013). Recently, we have implemented a TOPMODEL approach to model the hydrology following Niu et al. (2005). In this framework, we use a topographical index to infer subgrid hydrology (primarily the areal fraction of saturated soils). Similar to Ringeval et al. (2010), we make the assumption that only saturated soils (i.e. with a water table at, or above the surface) can contribute to methane emissions. This does not represent the whole complexity of methane emission dynamics (Bridgham et al., 2013), but it does account for the interannual variability of wet areas. However, because the global wetland extent and temporal variability are still poorly constrained, and because models produce very different estimates (Melton et al., 2013), we allow our methane model to use either its own diagnosed interactive wetland fraction estimate or the estimates from the Global Inundation Extent from Multi-Satellites (GIEMS) dataset (Prigent et al., 2007; Papa et al., 2010). The governing equation for methane production at depth z, in Hybrid8, is,

$$R_{CH_4} = R_0 \;\; Fps(z) C_{som}(z) Q_{10}^{T_{soil}(z)-T_0} \qquad (2)$$

Where R_0 is the baseline production rate; $Fps(z)$ is the maximum pore space fraction in a specific layer, which depends on soil texture; $C_{som}(z)$ is the Soil Organic Matter (SOM); $T_{soil}(z)$ is the soil temperature; Q_{10} is the temperature coefficient to account for the temperature dependency of methane flux; and $T_0 = 22\ ^\circ C$.

Q_{10} and R_0 are constant in time and homogeneous in space. We obtain $C_{som}(z)$ by running the model for 2500 years, reaching a quasi-equilibrium state. The model does not account for specific peatland-type ecosystems and running the model for a longer time (centuries to millennia) would have led to greater values in high northern latitudes (due to SOM building up). Ideally, it would have been better to run the same model (or a degraded version of it) over a complete glacial–interglacial cycle with interactive vegetation. However, the simplicity of our methane model is motivated by the recent findings of a consistent response curve to temperature from the microbial scale to the ecosystem scale (Yvon-Durocher et al., 2014). Our model has been compared to ground measurements and aircraft-based estimates in a recent study (O'Shea et al., 2014). Considering the large uncertainties in methane emission estimates (Melton et al., 2013), we choose to run our model for a range of possible R_0 (i.e. from $0.7\ 10^{-11}$ kg m^{-2} s^{-1} to $1.4\ 10^{-11}$ kg m^{-2} s^{-1}) and Q_{10} values (i.e. from 2 to 5). Present-day (i.e. 1991–2000) global mean annual emissions for our different model configurations are presented in Fig. 7. Hereafter the simulations resulting from this climate forcing will be referred as the "control experiment". In the following, we only consider the paired R_0/Q_{10} values resulting in global mean 1991–2000 annual emissions of 180 Tg ± 20%. Because there is a large discrepancy in the estimates of the wetland extent between the model and the GIEMS, the use of the different wetland estimates leads to different response curves of total emissions to model parameters. The model simulates wetlands mostly in and around the tropical band, with much less wetland area at high latitudes. Thus, the model fails to reproduce the large wetland areas of Siberia and North America. This mismatch between modelled wetlands and observations is shared with a number of surface models (Melton et al., 2013; Ringeval et al., 2014). Therefore, we expect the simulated emissions using the interactive wetlands to be more sensitive to changes happening around the tropics.

To simulate methane emissions during the LIG, we compute a set of four LIG climate anomalies from previous GCM (General Circulation Model) runs. The variables of interest in our case are monthly near surface air temperatures (absolute differences *LIG − Control*) and monthly total precipitation (relative differences *(LIG − Control)/Control*). We have used outputs from the following climate models:

- IPSL-CM4 (Braconnot et al., 2008; Marti et al., 2009)
- CNRM-CM3.3 (Salas-Mélia et al., 2005)
- CCSM4 (Merz et al., 2013)
- ECHAM5 (Fischer and Jungclaus, 2010)

We regenerated daily climatic forcings using the LIG GCM anomalies applied to the CRU monthly fields and performed 10 year simulations.

Fig. 8 shows the annual relative flux density changes for one particular methane model parameterisation under the different LIG climates. The flux density is the flux that would have been computed if the whole grid point was wetland and consequently the anomaly is mainly driven by temperature changes. The different climatic model forcings all produce a consistent increase in the flux density change at high northern latitudes, resulting from the increase of summer temperature in this area simulated by all four GCMs. However, in the tropics the different climatic forcings produce different flux density changes due to the large variability of the simulated temperature anomalies in these areas.

The methane emission is a result of the flux density, convolved with the wetland extent. We use two different wetland extent

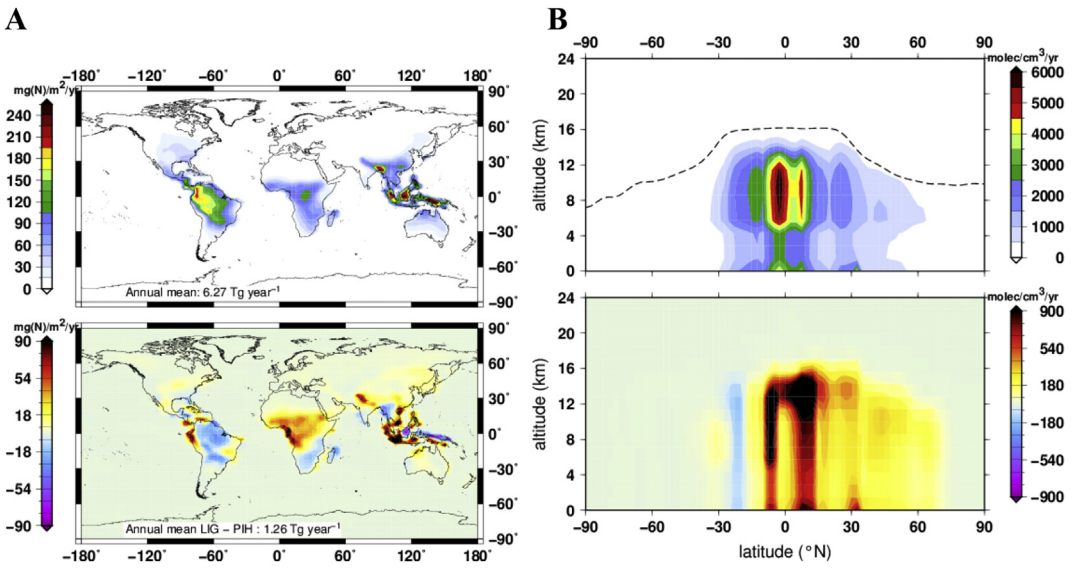

Fig. 6. **A**: Annual mean total column lightning-produced NOx (top) and relative change (*LIG-PIH*, bottom); **B**: Annual mean zonally averaged lightning-produced NOx (top) and relative change (*LIG-PIH*, bottom). The dashed line stands for the altitude of the tropopause diagnosed in the model.

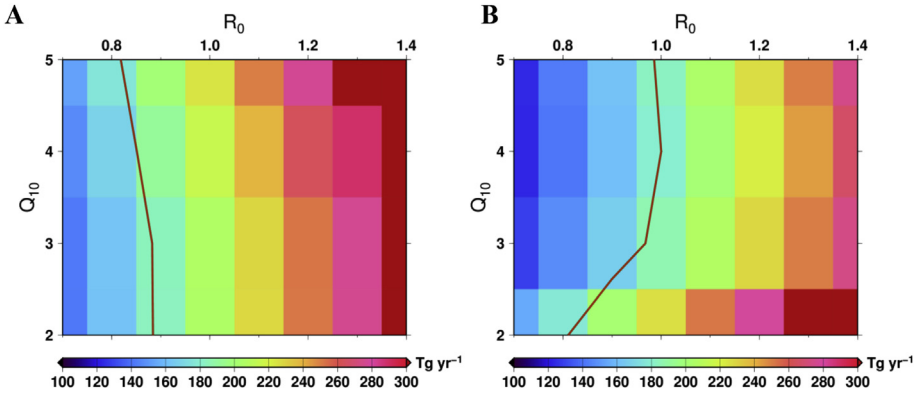

Fig. 7. Present day (1991–2000) simulated global mean annual emissions in the parameter (R_0, Q_{10}) space, using the interactive computations of wetland (**A**), or using the GIEMS product (**B**). The thick line shows the 180 Tg/yr isovalue (according to Table 1, pairs of R_0 and Q_{10} around this line should be favoured).

reconstructions for the LIG. First, we use the interactive wetland scheme of the model under the LIG climate. Second, we use the GIEMS dataset over which we superimposed a monthly wetland extent relative anomaly deduced from the model (*LIG − Control/Control*). We expect that the use of the relative anomaly superimposed to the GIEMS would limit the impact of possible model bias. At the global scale, the large variability between the GCM climates produce the following simulated methane emission ranges (Fig. 9):

- from −2% for IPSL4 to +10% for ECHAM5 in the interactive wetland mode, with a multi-model mean of +4%.
- from +11% for CCSM4 to +32% in IPSL4 using the GIEMS dataset (as is for the control run and with the modelled anomaly for the LIG), with a multi-model mean of +20.3%.

As expected, the use of different estimates of wetland extents has a strong impact on the relative methane response. The LIG warm anomaly is relatively limited to the tropical band, where most of the interactively computed wetlands lie, and it is far more pronounced in summer at high latitudes. This leads generally to greater impact of the LIG climatic anomalies when using the GIEMS estimates of wetlands.

Given the large uncertainties in the representation of wetland extent, it is tempting to use a fixed wetland mask (e.g. GIEMS) under a changing climate. In order to assess the importance of wetland extent responses to climate forcing, we also quantify the simulated change in wetlands between our two snapshot (control and LIG) model runs. For the four different GCM anomalies we only get a −1% to +2% change in the total wetland extent. However, the regional changes are significant (Fig. 10). In particular, the four GCM anomalies suggest a strengthening of the African and Indian monsoon, leading to an increase in the wetland extent there, consistent with palaeo records of vegetation (e.g. Frenzel et al., 1992; Frédoux, 1994; Farooqui et al., 2014) and ecosystem modelling (e.g. Nikolova et al., 2013). These regional changes have noticeable effects on the simulated emissions. Thus, as a sensitivity analysis, we compute the methane emission anomalies from the LIG compared to the control experiment using the exact same wetland extent between the two time slices. We use either the interactively modelled wetland extent with the control climatic forcing, or the GIEMS dataset. In both cases, we systematically

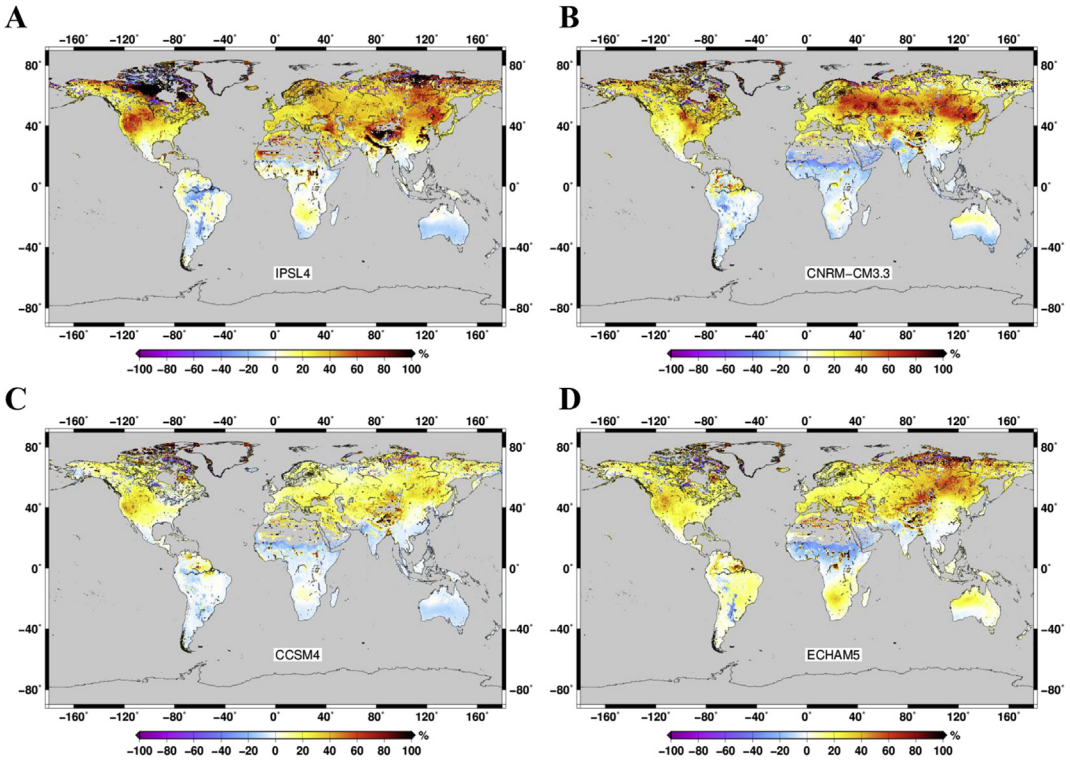

Fig. 8. Annual mean relative change (*LIG − Control*/*Control*) in the flux density (assuming 100% wetland fraction in grid cell) of methane emissions (for $R_0 = 0.9\ 10^{-11}$ kg m^{-2} s^{-1}; $Q_{10} = 3$): IPSL4 (**A**); CNRM-CM3.3 (**B**); CCSM4 (**C**), and ECHAM5 (**D**).

obtain lower estimates of methane emissions if we do not consider the change in wetland extent during the LIG (Table 5).

One caveat of our land surface simulations is that we use a fixed land sea mask. The sea level anomaly relative to present day was likely higher than 6.6 m at LIG peak insolation (Kopp et al., 2009). As a consequence, part of present-day low lands was submerged. From a methane perspective, this is mostly relevant in North America and Siberia. However, at the model scale (0.5°) this will result in a negligible change in the land-sea mask. For the same reason, we did not consider changing the ice sheet mask even though Greenland was likely reduced in size at this period of time. The most recent glaciological reconstructions tend to suggest a relatively limited melt of Greenland (e.g. Quiquet et al., 2013; Stone et al., 2013), justifying the fixed ice mask in our simulations. In addition, during the penultimate glaciation, the Saalian, the extent of the Eurasian ice sheet was much greater than during the LGM (e.g. Peltier, 2004; Svendsen et al., 2004). Thus, assuming similar topographical properties (topographical index) and soil properties (textures) during the LIG and during the PIH, is an approximation. However, to our knowledge, the effect of the Saalian ice sheets on

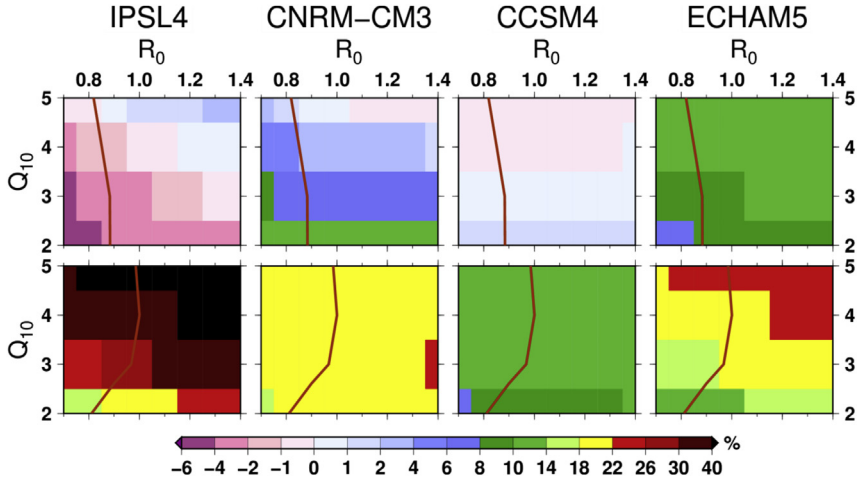

Fig. 9. Simulated LIG relative anomalies compared to the control simulation in mean annual emissions. Top panel: using interactive computation of wetlands; Bottom panel: using GIEMS dataset (as is for the control run and with the modelled anomaly for the LIG). The anomalies are computed using, respectively (left to right): IPSL4, CNRM3, CCSM4, and ECHAM5. The thick line show the 180 Tg/yr isovalue simulated emissions under present-day atmospheric forcings (here again, according to Table 1, pairs of R_0 and Q_{10} around this line should be favoured).

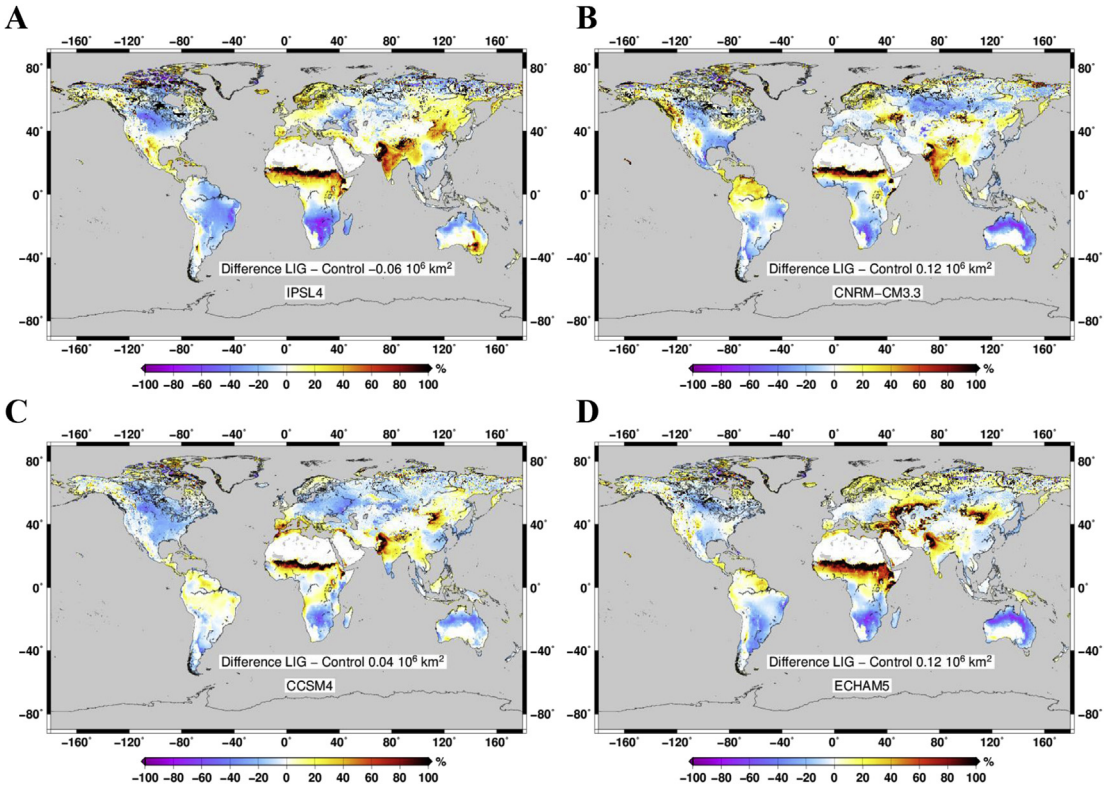

Fig. 10. Annual mean relative change (*LIG − Control/Control*) in wetland extent: IPSL4 (**A**); CNRM-CM3.3 (**B**); CCSM4 (**C**), and ECHAM5 (**D**). Absolute global extent difference is printed on each plot.

the landscape (isostasy and eroding work) is not yet quantified in the literature, and would require specific investigation beyond the scope of this work. Another important caveat is that we do not account for land cover change. There is evidence for regional vegetation changes through the LIG period (e.g. Tarasov et al., 2005; Velichko et al., 2005), which has also been assessed by ecosystem modelling in previous work (e.g. Harrison et al., 1995; Nikolova et al., 2013). In particular a northward shift of the boreal forest was simulated, as was a reduction in desert extent during the LIG (Nikolova et al., 2013). These changes could have had an important impact on the methane emissions, either through soil moisture feedbacks or changes in substrate availability. We suspect that our assumption of using modern day vegetation could lead to an underestimation of surface fluxes. We chose to ignore the sensitivity of methane emissions to vegetation, as biome classification reconstructions are relatively poorly constrained and models tend to display a large variability amongst them and a large sensitivity to atmospheric forcing, and consequently do not always match proxy data (e.g. Nikolova et al., 2013). We acknowledge the fact that this subject is of primary importance for understanding the source changes and it should be part of a rigorous study in the future.

Table 5
Methane emission anomalies resulting from the four different GCM anomalies. We present here the numbers for four different estimates of the wetland fractions: two reconstructed LIG wetland estimates, based on the absolute modelled wetlands and on the relative modelled wetlands applied to the GIEMS retrieval; and two simulations assuming no change in the wetland extents for the LIG compared to the control simulation. multi-satellite retrieval (being unchanged from Control to LIG); fully interactive model computation (different wetlands for Control and LIG); interactive model computation under the Control climate only (being unchanged from Control to LIG).

	LIG climate				Multi-model mean
	IPSL4	CNRM-CM3.3	CCSM4	ECHAM5	
LIG wetlands:					
Hybrid8, LIG climate	−2.1%	+6.3%	+0.0%	+10.3%	+3.6%
GIEMS + Hybrid8 anomalies	+31.7%	+19.7%	+11.1%	+18.6%	+20.3%
Control-forced wetlands:					
Hybrid8, Control climate	−3.5%	+1.8%	−2.5%	+7.2%	+0.8%
GIEMS	+15.7%	+8.8%	+4.8%	+9.7%	+9.8%

4. Conclusions

In this paper, we have reviewed much of the recent work that has quantified the relative importance of changes in methane sources and sinks during the Last Glacial–interglacial cycle. Measuring techniques are constantly improving and accuracy of the palaeo records has increased, allowing high precision analysis of the interpolar gradient for example. Models of both atmospheric chemistry and surface processes have been applied over this time period. Most modelling studies have quantified the source and sink changes from the LGM to PIH, with various degrees of agreement. Intercomparison exercises (for surface models see Melton et al., 2013; and (for atmospheric chemistry models see Naik et al., 2013; Voulgarakis et al., 2013)) are useful for diagnosing the reasons for the divergence. New processes (e.g. peatlands or hydrates) are currently being implemented in models and potential impacts of these on methane dynamics are being studied (e.g. Archer et al., 2009; Schuldt et al., 2013).

For the first time we have investigated in a comprehensive model framework, changes in methane sources and sinks during the Last Interglacial (LIG) period, the last warm period preceding our current interglacial. From an atmospheric perspective, we simulated a reduction in the methane lifetime during the LIG

compared to the PIH. Kinetics, water vapour, and lightning all contribute to decreasing the methane lifetime during the LIG. The temperature effect on NMVOC emissions to the contrary tends to moderately increase the lifetime, but the overall effect is a net decrease. However, we do not account for potential changes in soil moisture, vegetation distribution or leaf area index and our approach oversimplify the NMVOCs emitted. One improvement could be to use an interactive vegetation representation, with interactive isoprene emissions. The changes in the amount of NO_x produced by lightning are also clearly an important driver as they account for 18% of the lifetime reduction we simulate at the LIG relative to the PIH. An accurate representation of this process in large scale models is therefore essential for assessing changes in methane lifetime (e.g. Banerjee et al., 2014). However, changes in air temperature and humidity appear to constitute the dominant influence on the lifetime of methane during the LIG. For this reason, we think that one of the main caveats of our model simulations is that we have used only one set of oceanic conditions. Given the high variability in model reconstructions of the LIG period (Lunt et al., 2013a), it would have increased the robustness of our conclusions to test our results with various GCM oceanic boundary conditions. This should be investigated in future work. Finally, as part of future work we will test the importance of soil NO_x using an interactive biogenic emissions models, currently under development.

Regarding methane emissions, we simulated a slight increase in emissions from wetlands during the LIG but we did not explore changes in other, smaller sources such as biomass burning. For certain sets of model configuration, the increase in emissions could compensate the decrease in methane lifetime, leading to no change in methane mixing ratio. However, our results are relatively sensitive to atmospheric forcing fields and reflect the large uncertainties regarding LIG climate reconstructions. Further uncertainty arises from the definition of wetlands areas contributing to methane emissions. Thus, even if we do not simulate a drastic change in the global extent of wetlands, we do simulate regional changes which strongly influence the global estimate of emissions. Whilst present-day wetland estimates are still largely uncertain and poorly represented in models, their potential changes may greatly affect methane emissions. We conclude that this wetland distribution and its dynamics are therefore one of the most uncertain factors in methane models and should be carefully assessed during projections under future climate scenarios.

At a broader perspective, on the one hand, a fairly limited number of studies have evaluated chemistry–climate and surface models under palaeo-conditions. Most of them were performed during the 1990s and relied on relatively simple chemistry and/or treated limited feedbacks with climate. Since then, complexity has greatly improved and such models should be used as tools to investigate the response of trace gases under a changing climate. On the other hand, surface models provide lower boundary conditions the atmosphere needs. Most trace gas emissions are now process-based modelled. The association of atmosphere and surface models, coupled (ESM) or uncoupled (as in here), and its application under palaeo-conditions is now improving our ability to represent natural variability outside of present-day conditions (Lunt et al., 2013b).

Acknowledgements

We gratefully acknowledge I. Colin Prentice for his initial idea on this work. We also warmly acknowledge Antara Banerjee and Luke Abraham for having the UKCA-CheST model set up and running on HECToR supercomputer. We warmly thank Catherine Prigent for sharing her global inundation product. A.T.A., P.J.T and J.A.P. acknowledge NCAS climate for funding. A.T.A. was supported by a Herchel Smith fellowship. J.G.L. gratefully acknowledges support from the NERC funded CLAIRE-UK project. The research leading to these results has received funding from the European Community's Seventh Framework Programme (FP**7** 2007–2013) under grant agreement n° 238366. We acknowledge funding from the ERC under the ACCI project n° 267760. This work made use of the facilities of HECToR, the UK's national high-performance computing service, which is provided by UoE HPCx Ltd at the University of Edinburgh, Cray Inc and NAG Ltd, and funded by the Office of Science and Technology through EPSRC's High End Computing Programme. Part of this work was performed using the Darwin Supercomputer of the University of Cambridge High Performance Computing Service (http://www.hpc.cam.ac.uk/), provided by Dell Inc. using Strategic Research Infrastructure Funding from the Higher Education Funding Council for England and funding from the Science and Technology Facilities Council. Part of this work was carried out using the computational facilities of the Advanced Computing Research Centre, University of Bristol – http://www.bris.ac.uk/acrc/.

References

Anderson, P., Bermike, O., Bigelow, N., Brigham-Grette, J., Duvall, M., Edwards, M.E., Frechette, B., Funder, S., Johnsen, S., Knies, J., Koerner, R., Lozhkin, A., Marshall, S., Matthiessen, J., Macdonald, G., Miller, G., Montoya, M., Muhs, D., Otto-Bliesner, B., Overpeck, J., Reeh, N., Sejrup, H., Spielhagen, R., Turner, C., Velichko, A., 2006. Last Interglacial Arctic warmth confirms polar amplification of climate change. Quat. Sci. Rev. 25, 1383–1400.

Archer, D., Buffett, B., Brovkin, V., 2009. Ocean methane hydrates as a slow tipping point in the global carbon cycle. Proc. Natl. Acad. Sci. 106, 20596–20601. http://dx.doi.org/10.1073/pnas.0800885105.

Archibald, A.T., Levine, J.G., Abraham, N.L., Cooke, M.C., Edwards, P.M., Heard, D.E., Jenkin, M.E., Karunaharan, A., Pike, R.C., Monks, P.S., Shallcross, D.E., Telford, P.J., Whalley, L.K., Pyle, J.A., 2011. Impacts of HOx regeneration and recycling in the oxidation of isoprene: consequences for the composition of past, present and future atmospheres. Geophys. Res. Lett. 38 http://dx.doi.org/10.1029/2010GL046520.

Banerjee, A., Archibald, A.T., Maycock, A., Telford, P., Abraham, N.L., Yang, X., Braesicke, P., Pyle, J., 2014. Lightning NOx, a key chemistry–climate interaction: impacts of future climate change and consequences for tropospheric oxidising capacity. Atmos. Chem. Phys. Discuss. 14, 8753–8778. http://dx.doi.org/10.5194/acpd-14-8753-2014.

Baumgartner, M., Kindler, P., Eicher, O., Floch, G., Schilt, A., Schwander, J., Spahni, R., Capron, E., Chappellaz, J., Leuenberger, M., Fischer, H., Stocker, T.F., 2014. NGRIP CH_4 concentration from 120 to 10 kyr before present and its relation to a $\delta^{15}N$ temperature reconstruction from the same ice core. Clim. Past. 10, 903–920. http://dx.doi.org/10.5194/cp-10-903-2014.

Baumgartner, M., Schilt, A., Eicher, O., Schmitt, J., Schwander, J., Spahni, R., Fischer, H., Stocker, T.F., 2012. High-resolution interpolar difference of atmospheric methane around the Last Glacial Maximum. Biogeosciences 9, 3961–3977. http://dx.doi.org/10.5194/bg-9-3961-2012.

Blunier, T., Chappellaz, J., Schwander, J., Stauffer, B., Raynaud, D., 1995. Variations in atmospheric methane concentration during the Holocene epoch. Nature 374, 46–49. http://dx.doi.org/10.1038/374046a0.

Bock, J., Martinerie, P., Witrant, E., Chappellaz, J., 2012. Atmospheric impacts and ice core imprints of a methane pulse from clathrates. Earth Planet. Sci. Lett. 349–350, 98–108. http://dx.doi.org/10.1016/j.epsl.2012.06.052.

Bock, M., Schmitt, J., Möller, L., Spahni, R., Blunier, T., Fischer, H., 2010. Hydrogen isotopes preclude marine hydrate CH_4 emissions at the onset of Dansgaard–Oeschger events. Science 328, 1686–1689. http://dx.doi.org/10.1126/science.1187651.

Bousquet, P., Ciais, P., Miller, J.B., Dlugokencky, E.J., Hauglustaine, D.A., Prigent, C., Van der Werf, G.R., Peylin, P., Brunke, E.-G., Carouge, C., Langenfelds, R.L., Lathière, J., Papa, F., Ramonet, M., Schmidt, M., Steele, L.P., Tyler, S.C., White, J., 2006. Contribution of anthropogenic and natural sources to atmospheric methane variability. Nature 443, 439–443. http://dx.doi.org/10.1038/nature05132.

Braconnot, P., Marzin, C., Grégoire, L., Mosquet, E., Marti, O., 2008. Monsoon response to changes in Earth's orbital parameters: comparisons between simulations of the Eemian and of the Holocene. Clim. Past 4, 281–294. http://dx.doi.org/10.5194/cp-4-281-2008.

Bridgham, S.D., Cadillo-Quiroz, H., Keller, J.K., Zhuang, Q., 2013. Methane emissions from wetlands: biogeochemical, microbial, and modeling perspectives from local to global scales. Glob. Change Biol. 19, 1325–1346. http://dx.doi.org/10.1111/gcb.12131.

Brook, E.J., Harder, S., Severinghaus, J., Steig, E.J., Sucher, C.M., 2000. On the origin and timing of rapid changes in atmospheric methane during the Last Glacial

Period. Glob. Biogeochem. Cycles 14, 559–572. http://dx.doi.org/10.1029/1999GB001182.
Burns, S.J., 2011. Speleothem records of changes in tropical hydrology over the Holocene and possible implications for atmospheric methane. Holocene 21, 735–741. http://dx.doi.org/10.1177/0959683611400194.
Capron, E., Govin, A., Stone, E.J., Masson-Delmotte, V., Mulitza, S., Otto-Bliesner, B., Rasmussen, T.L., Sime, L.C., Waelbroeck, C., Wolff, E.W., 2014. Temporal and spatial structure of multi-millennial temperature changes at high latitudes during the Last Interglacial. Quat. Sci. Rev. 103, 116–133. http://dx.doi.org/10.1016/j.quascirev.2014.08.018.
Chappellaz, J.A., Fung, I.Y., Thompson, A.M., 1993. The atmospheric CH_4 increase since the Last Glacial Maximum. Tellus B 45, 228–241. http://dx.doi.org/10.1034/j.1600-0889.1993.t01-2-00002.x.
Chappellaz, J., Barnola, J.M., Raynaud, D., Lorius, C., Korotkevich, Y.S., 1990. Ice-core record of atmospheric methane over the past 160,000 years. Nature 345, 127–131. http://dx.doi.org/10.1038/345127a0.
Chappellaz, J., Blunier, T., Kints, S., Dällenbach, A., Barnola, J.-M., Schwander, J., Raynaud, D., Stauffer, B., 1997. Changes in the atmospheric CH_4 gradient between Greenland and Antarctica during the Holocene. J. Geophys. Res. Atmos. 102, 15987–15997. http://dx.doi.org/10.1029/97JD01017.
Chappellaz, J., Stowasser, C., Blunier, T., Baslev-Clausen, D., Brook, E.J., Dallmayr, R., Faïn, X., Lee, J.E., Mitchell, L.E., Pascual, O., Romanini, D., Rosen, J., Schüpbach, S., 2013. High-resolution glacial and deglacial record of atmospheric methane by continuous-flow and laser spectrometer analysis along the NEEM ice core. Clim. Past 9, 2579–2593. http://dx.doi.org/10.5194/cp-9-2579-2013.
Christensen, T.R., Ekberg, A., Ström, L., Mastepanov, M., Panikov, N., Öquist, M., Svensson, B.H., Nykänen, H., Martikainen, P.J., Oskarsson, H., 2003. Factors controlling large scale variations in methane emissions from wetlands. Geophys. Res. Lett. 30 http://dx.doi.org/10.1029/2002GL016848.
Craig, H., Chou, C.C., 1982. Methane: the record in polar ice cores. Geophys. Res. Lett. 9, 1221–1224. http://dx.doi.org/10.1029/GL009i011p01221.
Crutzen, P.J., Brühl, C., 1993. A model study of atmospheric temperatures and the concentrations of ozone, hydroxyl, and some other photochemically active gases during the glacial, the pre-industrial Holocene and the present. Geophys. Res. Lett. 20, 1047–1050. http://dx.doi.org/10.1029/93GL01423.
Dällenbach, A., Blunier, T., Flückiger, J., Stauffer, B., Chappellaz, J., Raynaud, D., 2000. Changes in the atmospheric CH_4 gradient between Greenland and Antarctica during the Last Glacial and the transition to the Holocene. Geophys. Res. Lett. 27, 1005–1008. http://dx.doi.org/10.1029/1999GL010873.
Farooqui, A., Pattan, J.N., Parthiban, G., Srivastava, J., Ranjana, 2014. Palynological record of tropical rain forest vegetation and sea level fluctuations since 140 ka from sediment core, south-eastern Arabian Sea. Palaeogeogr. Palaeoclimatol. Palaeoecol. 411, 95–109. http://dx.doi.org/10.1016/j.palaeo.2014.06.020.
Fischer, H., Behrens, M., Bock, M., Richter, U., Schmitt, J., Loulergue, L., Chappellaz, J., Spahni, R., Blunier, T., Leuenberger, M., Stocker, T.F., 2008. Changing boreal methane sources and constant biomass burning during the last termination. Nature 452, 864–867. http://dx.doi.org/10.1038/nature06825.
Fischer, N., Jungclaus, J.H., 2010. Effects of orbital forcing on atmosphere and ocean heat transports in Holocene and Eemian climate simulations with a comprehensive Earth system model. Clim. Past 6, 155–168. http://dx.doi.org/10.5194/cp-6-155-2010.
Frédoux, A., 1994. Pollen analysis of a deep-sea core in the Gulf of Guinea: vegetation and climatic changes during the last 225,000 years B.P. Palaeogeogr. Palaeoclimatol. Palaeoecol. Pollen Clim. 109, 317–330. http://dx.doi.org/10.1016/0031-0182(94)90182-1.
Frenzel, B., Pécsi, M., Velichko, A.A., 1992. Atlas of Paleoclimates and Paleoenvironments of the Northern Hemisphere. Late Pleistocene–Holocene. Verlag, Budapest-Stuttgart.
Friend, A.D., 1998. Parameterisation of a global daily weather generator for terrestrial ecosystem modelling. Ecol. Model 109, 121–140. http://dx.doi.org/10.1016/S0304-3800(98)00036-2.
Friend, A.D., Kiang, N.Y., 2005. Land surface model development for the GISS GCM: effects of improved canopy physiology on simulated climate. J. Clim. 18, 2883–2902. http://dx.doi.org/10.1175/JCLI3425.1.
Guenther, A.B., Jiang, X., Heald, C.L., Sakulyanontvittaya, T., Duhl, T., Emmons, L.K., Wang, X., 2012. The Model of Emissions of Gases and Aerosols from nature version 2.1 (MEGAN2.1): an extended and updated framework for modeling biogenic emissions. Geosci. Model Dev. 5, 1471–1492. http://dx.doi.org/10.5194/gmd-5-1471-2012.
Guenther, A., Karl, T., Harley, P., Wiedinmyer, C., Palmer, P.I., Geron, C., 2006. Estimates of global terrestrial isoprene emissions using MEGAN (Model of Emissions of Gases and Aerosols from Nature). Atmos. Chem. Phys. 6, 3181–3210. http://dx.doi.org/10.5194/acp-6-3181-2006.
Harder, S.L., Shindell, D.T., Schmidt, G.A., Brook, E.J., 2007. A global climate model study of CH_4 emissions during the Holocene and glacial–interglacial transitions constrained by ice core data. Glob. Biogeochem. Cycles 21. http://dx.doi.org/10.1029/2005GB002680.
Harris, I., Jones, P. d., Osborn, T. j., Lister, D. h, 2013. Updated high-resolution grids of monthly climatic observations – the CRU TS3.10 Dataset. Int. J. Climatol. http://dx.doi.org/10.1002/joc.3711.
Harrison, S.P., Kutzbach, J.E., Prentice, I.C., Behling, P.J., Sykes, M.T., 1995. The response of northern hemisphere extratropical climate and vegetation to orbitally induced changes in insolation during the Last Interglaciation. Quat. Res. 43, 174–184. http://dx.doi.org/10.1006/qres.1995.1018.
Holmes, C.D., Prather, M.J., Søvde, O.A., Myhre, G., 2013. Future methane, hydroxyl, and their uncertainties: key climate and emission parameters for future predictions. Atmos. Chem. Phys. 13, 285–302. http://dx.doi.org/10.5194/acp-13-285-2013.
Hopcroft, P.O., Valdes, P.J., Beerling, D.J., 2011. Simulating idealized Dansgaard–Oeschger events and their potential impacts on the global methane cycle. Quat. Sci. Rev. 30, 3258–3268. http://dx.doi.org/10.1016/j.quascirev.2011.08.012.
Hopcroft, P.O., Valdes, P.J., Wania, R., Beerling, D.J., 2014. Limited response of peatland CH_4 emissions to abrupt Atlantic Ocean circulation changes in glacial climates. Clim. Past 10, 137–154. http://dx.doi.org/10.5194/cp-10-137-2014.
Jackowicz-Korczyński, M., Christensen, T.R., Bäckstrand, K., Crill, P., Friborg, T., Mastepanov, M., Ström, L., 2010. Annual cycle of methane emission from a subarctic peatland. J. Geophys. Res. Biogeosci. 115 http://dx.doi.org/10.1029/2008JG000913.
Kaplan, J.O., 2002. Wetlands at the Last Glacial Maximum: distribution and methane emissions. Geophys. Res. Lett. 29, 3-1–3-4. http://dx.doi.org/10.1029/2001GL013366.
Kaplan, J.O., Folberth, G., Hauglustaine, D.A., 2006. Role of methane and biogenic volatile organic compound sources in late glacial and Holocene fluctuations of atmospheric methane concentrations. Glob. Biogeochem. Cycles 20. http://dx.doi.org/10.1029/2005GB002590.
Karol, I.L., Frolkis, V.A., Kiselev, A.A., 1995. Radiative-photochemical modeling of the annually averaged composition and temperature of the global atmosphere during the last glacial and interglacial periods. J. Geophys. Res. Atmos. 100, 7291–7301. http://dx.doi.org/10.1029/94JD02385.
Keeling, C.D., Bacastow, R.B., Bainbridge, A.E., Ekdahl, C.A., Guenther, P.R., Waterman, L.S., Chin, J.F.S., 1976. Atmospheric carbon dioxide variations at Mauna Loa Observatory, Hawaii. Tellus 28, 538–551. http://dx.doi.org/10.1111/j.2153-3490.1976.tb00701.x.
Kennett, J.P., Cannariato, K.G., Hendy, I.L., Behl, R.J., 2003. Methane Hydrates in Quaternary Climate Change: the Clathrate Gun Hypothesis. American Geophysical Union, Washington, D. C.
Khalil, M.A.K., Rasmussen, R.A., 1985. Causes of increasing atmospheric methane: depletion of hydroxyl radicals and the rise of emissions. Atmos. Environ. 1967 19, 397–407. http://dx.doi.org/10.1016/0004-6981(85)90161-1.
Kirschke, S., Bousquet, P., Ciais, P., Saunois, M., Canadell, J.G., Dlugokencky, E.J., Bergamaschi, P., Bergmann, D., Blake, D.R., Bruhwiler, L., Cameron-Smith, P., Castaldi, S., Chevallier, F., Feng, L., Fraser, A., Heimann, M., Hodson, E.L., Houweling, S., Josse, B., Fraser, P.J., Krummel, P.B., Lamarque, J.-F., Langenfelds, R.L., Le Quéré, C., Naik, V., O'Doherty, S., Palmer, P.I., Pison, I., Plummer, D., Poulter, B., Prinn, R.G., Rigby, M., Ringeval, B., Santini, M., Schmidt, M., Shindell, D.T., Simpson, I.J., Spahni, R., Steele, L.P., Strode, S.A., Sudo, K., Szopa, S., van der Werf, G.R., Voulgarakis, A., van Weele, M., Weiss, R.F., Williams, J.E., Zeng, G., 2013. Three decades of global methane sources and sinks. Nat. Geosci. 6, 813–823. http://dx.doi.org/10.1038/ngeo1955.
Kleinen, T., Brovkin, V., Schuldt, R.J., 2012. A dynamic model of wetland extent and peat accumulation: results for the Holocene. Biogeosciences 9, 235–248. http://dx.doi.org/10.5194/bg-9-235-2012.
Konijnendijk, T.Y.M., Weber, S.L., Tuenter, E., van Weele, M., 2011. Methane variations on orbital timescales: a transient modeling experiment. Clim. Past 7, 635–648. http://dx.doi.org/10.5194/cp-7-635-2011.
Kopp, R.E., Simons, F.J., Mitrovica, J.X., Maloof, A.C., Oppenheimer, M., 2009. Probabilistic assessment of sea level during the last interglacial stage. Nature 462, 863–867. http://dx.doi.org/10.1038/nature08686.
Kutzbach, J.E., 1981. Monsoon climate of the Early Holocene: climate experiment with the Earth's orbital parameters for 9000 years ago. Science 214, 59–61. http://dx.doi.org/10.1126/science.214.4516.59.
Lamarque, J.-F., Bond, T.C., Eyring, V., Granier, C., Heil, A., Klimont, Z., Lee, D., Liousse, C., Mieville, A., Owen, B., Schultz, M.G., Shindell, D., Smith, S.J., Stehfest, E., Van Aardenne, J., Cooper, O.R., Kainuma, M., Mahowald, N., McConnell, J.R., Naik, V., Riahi, K., van Vuuren, D.P., 2010. Historical (1850–2000) gridded anthropogenic and biomass burning emissions of reactive gases and aerosols: methodology and application. Atmos. Chem. Phys. 10, 7017–7039. http://dx.doi.org/10.5194/acp-10-7017-2010.
Landais, A., Caillon, N., Goujon, C., Grachev, A.M., Barnola, J.M., Chappellaz, J., Jouzel, J., Masson-Delmotte, V., Leuenberger, M., 2004. Quantification of rapid temperature change during DO event 12 and phasing with methane inferred from air isotopic measurements. Earth Planet. Sci. Lett. 225, 221–232. http://dx.doi.org/10.1016/j.epsl.2004.06.009.
Lawson, I.T., Tzedakis, P.C., Roucoux, K.H., Galanidou, N., 2013. The anthropogenic influence on wildfire regimes: charcoal records from the Holocene and Last Interglacial at Ioannina, Greece. J. Biogeogr. 40, 2324–2334. http://dx.doi.org/10.1111/jbi.12164.
Levine, J.G., Wolff, E.W., Hopcroft, P.O., Valdes, P.J., 2012. Controls on the tropospheric oxidizing capacity during an idealized Dansgaard–Oeschger event, and their implications for the rapid rises in atmospheric methane during the last glacial period. Geophys. Res. Lett. 39 http://dx.doi.org/10.1029/2012GL051866.
Levine, J.G., Wolff, E.W., Jones, A.E., Sime, L.C., 2011a. The role of atomic chlorine in glacial-interglacial changes in the carbon-13 content of atmospheric methane. Geophys. Res. Lett. 38, L04801. http://dx.doi.org/10.1029/2010GL046122.
Levine, J.G., Wolff, E.W., Jones, A.E., Sime, L.C., Valdes, P.J., Archibald, A.T., Carver, G.D., Warwick, N.J., Pyle, J.A., 2011b. Reconciling the changes in atmospheric methane sources and sinks between the Last Glacial Maximum and the

pre-industrial era. Geophys. Res. Lett. 38 http://dx.doi.org/10.1029/2011GL049545.
Loulergue, L., Schilt, A., Spahni, R., Masson-Delmotte, V., Blunier, T., Lemieux, B., Barnola, J.-M., Raynaud, D., Stocker, T.F., Chappellaz, J., 2008. Orbital and millennial-scale features of atmospheric CH_4 over the past 800,000 years. Nature 453, 383–386. http://dx.doi.org/10.1038/nature06950.
Lunt, D.J., Abe-Ouchi, A., Bakker, P., Berger, A., Braconnot, P., Charbit, S., Fischer, N., Herold, N., Jungclaus, J.H., Khon, V.C., Krebs-Kanzow, U., Langebroek, P.M., Lohmann, G., Nisancioglu, K.H., Otto-Bliesner, B.L., Park, W., Pfeiffer, M., Phipps, S.J., Prange, M., Rachmayani, R., Renssen, H., Rosenbloom, N., Schneider, B., Stone, E.J., Takahashi, K., Wei, W., Yin, Q., Zhang, Z.S., 2013a. A multi-model assessment of last interglacial temperatures. Clim. Past 9, 699–717. http://dx.doi.org/10.5194/cp-9-699-2013.
Lunt, D.J., Elderfield, H., Pancost, R., Ridgwell, A., Foster, G.L., Haywood, A., Kiehl, J., Sagoo, N., Shields, C., Stone, E.J., Valdes, P., 2013b. Warm climates of the past—a lesson for the future? Philos. Trans. R. Soc. Math. Phys. Eng. Sci. 371, 20130146. http://dx.doi.org/10.1098/rsta.2013.0146.
Lu, Y., Khalil, M.A.K., 1991. Tropospheric OH: model calculations of spatial, temporal, and secular variations. Chemosphere 23, 397–444. http://dx.doi.org/10.1016/0045-6535(91)90194-I.
MacFarling Meure, C., Etheridge, D., Trudinger, C., Steele, P., Langenfelds, R., van Ommen, T., Smith, A., Elkins, J., 2006. Law Dome CO_2, CH_4 and N_2O ice core records extended to 2000 years BP. Geophys. Res. Lett. 33, L14810. http://dx.doi.org/10.1029/2006GL026152.
Martinerie, P., Brasseur, G.P., Granier, C., 1995. The chemical composition of ancient atmospheres: a model study constrained by ice core data. J. Geophys. Res. Atmos. 100, 14291–14304. http://dx.doi.org/10.1029/95JD00826.
Marti, O., Braconnot, P., Dufresne, J.-L., Bellier, J., Benshila, R., Bony, S., Brockmann, P., Cadule, P., Caubel, A., Codron, F., Noblet, N., Denvil, S., Fairhead, L., Fichefet, T., Foujols, M.-A., Friedlingstein, P., Goosse, H., Grandpeix, J.-Y., Guilyardi, E., Hourdin, F., Idelkadi, A., Kageyama, M., Krinner, G., Lévy, C., Madec, G., Mignot, J., Musat, I., Swingedouw, D., Talandier, C., 2009. Key features of the IPSL ocean atmosphere model and its sensitivity to atmospheric resolution. Clim. Dyn. 34, 1–26. http://dx.doi.org/10.1007/s00382-009-0640-6.
Maslin, M., Owen, M., Betts, R., Day, S., Jones, T.D., Ridgwell, A., 2010. Gas hydrates: past and future geohazard? Philos. Trans. R. Soc. Math. Phys. Eng. Sci. 368, 2369–2393. http://dx.doi.org/10.1098/rsta.2010.0065.
McElroy, M.B., 1989. Studies of Polar Ice: Insights for Atmospheric Chemistry. Rep. Dahl. Workshop Environ. Rec. Glaciers Ice Sheets 379.
Melton, J.R., Schaefer, H., Whiticar, M.J., 2012. Enrichment in ^{13}C of atmospheric CH_4 during the Younger Dryas termination. Clim. Past 8, 1177–1197. http://dx.doi.org/10.5194/cp-8-1177-2012.
Melton, J.R., Wania, R., Hodson, E.L., Poulter, B., Ringeval, B., Spahni, R., Bohn, T., Avis, C.A., Beerling, D.J., Chen, G., Eliseev, A.V., Denisov, S.N., Hopcroft, P.O., Lettenmaier, D.P., Riley, W.J., Singarayer, J.S., Subin, Z.M., Tian, H., Zürcher, S., Brovkin, V., van Bodegom, P.M., Kleinen, T., Yu, Z.C., Kaplan, J.O., 2013. Present state of global wetland extent and wetland methane modelling: conclusions from a model inter-comparison project (WETCHIMP). Biogeosciences 10, 753–788. http://dx.doi.org/10.5194/bg-10-753-2013.
Merz, N., Raible, C.C., Fischer, H., Varma, V., Prange, M., Stocker, T.F., 2013. Greenland accumulation and its connection to the large-scale atmospheric circulation in ERA-Interim and paleoclimate simulations. Clim. Past 9, 2433–2450. http://dx.doi.org/10.5194/cp-9-2433-2013.
Mischler, J.A., Sowers, T.A., Alley, R.B., Battle, M., McConnell, J.R., Mitchell, L., Popp, T., Sofen, E., Spencer, M.K., 2009. Carbon and hydrogen isotopic composition of methane over the last 1000 years. Glob. Biogeochem. Cycles 23. http://dx.doi.org/10.1029/2009GB003460.
Mitchell, L., Brook, E., Lee, J.E., Buizert, C., Sowers, T., 2013. Constraints on the Late Holocene anthropogenic contribution to the atmospheric methane budget. Science 342, 964–966. http://dx.doi.org/10.1126/science.1238920.
Möller, L., Sowers, T., Bock, M., Spahni, R., Behrens, M., Schmitt, J., Miller, H., Fischer, H., 2013. Independent variations of CH_4 emissions and isotopic composition over the past 160,000 years. Nat. Geosci. 6, 885–890. http://dx.doi.org/10.1038/ngeo1922.
Morgenstern, O., Braesicke, P., O'Connor, F.M., Bushell, A.C., Johnson, C.E., Osprey, S.M., Pyle, J.A., 2009. Evaluation of the new UKCA climate-composition model – part 1: the stratosphere. Geosci. Model Dev. 2, 43–57. http://dx.doi.org/10.5194/gmd-2-43-2009.
Murray, L.T., Logan, J.A., Jacob, D.J., 2013. Interannual variability in tropical tropospheric ozone and OH: the role of lightning. J. Geophys. Res. Atmos. 118, 11,468–11,480. http://dx.doi.org/10.1002/jgrd.50857.
Murray, L.T., Mickley, L.J., Kaplan, J.O., Sofen, E.D., Pfeiffer, M., Alexander, B., 2014. Factors controlling variability in the oxidative capacity of the troposphere since the Last Glacial Maximum. Atmos. Chem. Phys. 14, 3589–3622. http://dx.doi.org/10.5194/acp-14-3589-2014.
Naik, V., Voulgarakis, A., Fiore, A.M., Horowitz, L.W., Lamarque, J.-F., Lin, M., Prather, M.J., Young, P.J., Bergmann, D., Cameron-Smith, P.J., Cionni, I., Collins, W.J., Dalsøren, S.B., Doherty, R., Eyring, V., Faluvegi, G., Folberth, G.A., Josse, B., Lee, Y.H., MacKenzie, I.A., Nagashima, T., van Noije, T.P.C., Plummer, D.A., Righi, M., Rumbold, S.T., Skeie, R., Shindell, D.T., Stevenson, D.S., Strode, S., Sudo, K., Szopa, S., Zeng, G., 2013. Preindustrial to present-day changes in tropospheric hydroxyl radical and methane lifetime from the Atmospheric Chemistry and Climate Model Intercomparison Project (ACCMIP). Atmos. Chem. Phys. 13, 5277–5298. http://dx.doi.org/10.5194/acp-13-5277-2013.
NEEM Members, 2013. Eemian interglacial reconstructed from a Greenland folded ice core. Nature 493, 489–494. http://dx.doi.org/10.1038/nature11789.
Nikolova, I., Yin, Q., Berger, A., Singh, U.K., Karami, M.P., 2013. The last interglacial (Eemian) climate simulated by LOVECLIM and CCSM3. Clim. Past 9, 1789–1806. http://dx.doi.org/10.5194/cp-9-1789-2013.
Nisbet, E.G., 1992. Sources of atmospheric CH_4 in early postglacial time. J. Geophys. Res. Atmos. 97, 12859–12867. http://dx.doi.org/10.1029/92JD00743.
Nisbet, E.G., Chappellaz, J., 2009. Shifting gear, quickly. Science 324, 477–478. http://dx.doi.org/10.1126/science.1172001.
Niu, G.-Y., Yang, Z.-L., Dickinson, R.E., Gulden, L.E., 2005. A simple TOPMODEL-based runoff parameterization (SIMTOP) for use in global climate models. J. Geophys. Res. Atmos. 110 http://dx.doi.org/10.1029/2005JD006111.
O'Connor, F.M., Johnson, C.E., Morgenstern, O., Abraham, N.L., Braesicke, P., Dalvi, M., Folberth, G.A., Sanderson, M.G., Telford, P.J., Voulgarakis, A., Young, P.J., Zeng, G., Collins, W.J., Pyle, J.A., 2014. Evaluation of the new UKCA climate-composition model – part 2: the troposphere. Geosci. Model Dev. 7, 41–91. http://dx.doi.org/10.5194/gmd-7-41-2014.
O'Shea, S.J., Allen, G., Gallagher, M.W., Bower, K., Illingworth, S.M., Muller, J.B.A., Jones, B., Percival, C.J., Bauguitte, S.J.-B., Cain, M., Warwick, N., Quiquet, A., Skiba, U., Drewer, J., Dinsmore, K., Nisbet, E.G., Lowry, D., Fisher, R.E., France, J.L., Aurela, M., Lohila, A., Hayman, G., George, C., Clark, D., Manning, A.J., Friend, A.D., Pyle, J., 2014. Methane and carbon dioxide fluxes and their regional scalability for the European Arctic wetlands during the MAMM project in summer 2012. Atmos. Chem. Phys. Discuss. 14, 8455–8494, Available at: http://www.atmos-chem-phys.net/14/13159/2014/acp-14-13159-2014.html, http://dx.doi.org/10.5194/acpd-14-8455-2014.
Papa, F., Prigent, C., Aires, F., Jimenez, C., Rossow, W.B., Matthews, E., 2010. Interannual variability of surface water extent at the global scale, 1993–2004. J. Geophys. Res. Atmos. 115 http://dx.doi.org/10.1029/2009JD012674.
Peltier, W.R., 2004. GLOBAL glacial isostasy and the surface of the ice-age EARTH: the ICE-5G (VM2) model and GRACE. Annu. Rev. Earth Planet. Sci. 32, 111–149. http://dx.doi.org/10.1146/annurev.earth.32.082503.144359.
Petit, J.R., Jouzel, J., Raynaud, D., Barkov, N.I., Barnola, J.-M., Basile, I., Bender, M., Chappellaz, J., Davis, M., Delaygue, G., Delmotte, M., Kotlyakov, V.M., Legrand, M., Lipenkov, V.Y., Lorius, C., PÉpin, L., Ritz, C., Saltzman, E., Stievenard, M., 1999. Climate and atmospheric history of the past 420,000 years from the Vostok ice core, Antarctica. Nature 399, 429–436. http://dx.doi.org/10.1038/20859.
Petrenko, V.V., Smith, A.M., Brook, E.J., Lowe, D., Riedel, K., Brailsford, G., Hua, Q., Schaefer, H., Reeh, N., Weiss, R.F., Etheridge, D., Severinghaus, J.P., 2009. $^{14}CH_4$ measurements in Greenland Ice: investigating last glacial termination CH_4 sources. Science 324, 506–508. http://dx.doi.org/10.1126/science.1168909.
Pinto, J.P., Khalil, M. a. K., 1991. The stability of tropospheric OH during ice ages, inter-glacial epochs and modern times. Tellus B 43, 347–352. http://dx.doi.org/10.1034/j.1600-0889.1991.t01-2-00001.x.
Power, M.J., Marlon, J., Ortiz, N., Bartlein, P.J., Harrison, S.P., Mayle, F.E., Ballouche, A., Bradshaw, R.H.W., Carcaillet, C., Cordova, C., Mooney, S., Moreno, P.I., Prentice, I.C., Thonicke, K., Tinner, W., Whitlock, C., Zhang, Y., Zhao, Y., Ali, A.A., Anderson, R.S., Beer, R., Behling, H., Briles, C., Brown, K.J., Brunelle, A., Bush, M., Camill, P., Chu, G.Q., Clark, J., Colombaroli, D., Connor, S., Daniau, A.-L., Daniels, M., Dodson, J., Doughty, E., Edwards, M.E., Finsinger, W., Foster, D., Frechette, J., Gaillard, M.-J., Gavin, D.G., Gobet, E., Haberle, S., Hallett, D.J., Higuera, P., Hope, G., Horn, S., Inoue, J., Kaltenrieder, P., Kennedy, L., Kong, Z.C., Larsen, C., Long, C.J., Lynch, J., Lynch, E.A., McGlone, M., Meeks, S., Mensing, S., Meyer, G., Minckley, T., Mohr, J., Nelson, D.M., New, J., Newnham, R., Noti, R., Oswald, W., Pierce, J., Richard, P.J.H., Rowe, C., Goñi, M.F.S., Shuman, B.N., Takahara, H., Toney, J., Turney, C., Urrego-Sanchez, D.H., Umbanhowar, C., Vandergoes, M., Vanniere, B., Vescovi, E., Walsh, M., Wang, X., Williams, N., Wilmshurst, J., Zhang, J.H., 2008. Changes in fire regimes since the Last Glacial Maximum: an assessment based on a global synthesis and analysis of charcoal data. Clim. Dyn. 30, 887–907. http://dx.doi.org/10.1007/s00382-007-0334-x.
Power, M.J., Marlon, J.R., Bartlein, P.J., Harrison, S.P., 2010. Fire history and the Global Charcoal Database: a new tool for hypothesis testing and data exploration. Palaeogeogr. Palaeoclimatol. Palaeoecol. 291, 52–59. http://dx.doi.org/10.1016/j.palaeo.2009.09.014.
Prather, M.J., 2007. Lifetimes and time scales in atmospheric chemistry. Philos. Trans. R. Soc. Math. Phys. Eng. Sci. 365, 1705–1726. http://dx.doi.org/10.1098/rsta.2007.2040.
Price, C., Rind, D., 1994. Modeling global lightning distributions in a general circulation model. Mon. Weather Rev. 122, 1930–1939. http://dx.doi.org/10.1175/1520-0493(1994)122<1930:MGLDIA>2.0.CO;2.
Prigent, C., Papa, F., Aires, F., Rossow, W.B., Matthews, E., 2007. Global inundation dynamics inferred from multiple satellite observations, 1993–2000. J. Geophys. Res. Atmos. 112 http://dx.doi.org/10.1029/2006JD007847.
Quiquet, A., Ritz, C., Punge, H.J., Salas y Mélia, D., 2013. Greenland ice sheet contribution to sea level rise during the last interglacial period: a modelling study driven and constrained by ice core data. Clim. Past 9, 353–366. http://dx.doi.org/10.5194/cp-9-353-2013.
Raynaud, D., Chappellaz, J., Barnola, J.M., Korotkevich, Y.S., Lorius, C., 1988. Climatic and CH_4 cycle implications of glacial–interglacial CH_4 change in the Vostok ice core. Nature 333, 655–657. http://dx.doi.org/10.1038/333655a0.
Rayner, N.A., Parker, D.E., Horton, E.B., Folland, C.K., Alexander, L.V., Rowell, D.P., Kent, E.C., Kaplan, A., 2003. Global analyses of sea surface temperature, sea ice,

and night marine air temperature since the late nineteenth century. J. Geophys. Res. Atmos. 108, 4407. http://dx.doi.org/10.1029/2002JD002670.
Reagan, M.T., Moridis, G.J., 2007. Oceanic gas hydrate instability and dissociation under climate change scenarios. Geophys. Res. Lett. 34 http://dx.doi.org/10.1029/2007GL031671.
Ringeval, B., de Noblet-Ducoudré, N., Ciais, P., Bousquet, P., Prigent, C., Papa, F., Rossow, W.B., 2010. An attempt to quantify the impact of changes in wetland extent on methane emissions on the seasonal and interannual time scales. Glob. Biogeochem. Cycles 24. http://dx.doi.org/10.1029/2008GB003354.
Ringeval, B., Hopcroft, P.O., Valdes, P.J., Ciais, P., Ramstein, G., Dolman, A.J., Kageyama, M., 2013. Response of methane emissions from wetlands to the Last Glacial Maximum and an idealized Dansgaard–Oeschger climate event: insights from two models of different complexity. Clim. Past 9, 149–171. http://dx.doi.org/10.5194/cp-9-149-2013.
Ringeval, B., Houweling, S., van Bodegom, P.M., Spahni, R., van Beek, R., Joos, F., Röckmann, T., 2014. Methane emissions from floodplains in the Amazon Basin: challenges in developing a process-based model for global applications. Biogeosciences 11, 1519–1558. http://dx.doi.org/10.5194/bg-11-1519-2014.
Robbins, R.C., Cavanagh, L.A., Salas, L.J., Robinson, E., 1973. Analysis of ancient atmospheres. J. Geophys. Res. 78, 5341–5344. http://dx.doi.org/10.1029/JC078i024p05341.
Rosen, J.L., Brook, E.J., Severinghaus, J.P., Blunier, T., Mitchell, L.E., Lee, J.E., Edwards, J.S., Gkinis, V., 2014. An ice core record of near-synchronous global climate changes at the Bolling transition. Nat. Geosci. 7, 459–463. http://dx.doi.org/10.1038/ngeo2147.
Ruddiman, W.F., 2003. The anthropogenic greenhouse era began thousands of years ago. Clim. Change 61, 261–293. http://dx.doi.org/10.1023/B:CLIM.0000004577.17928.fa.
Salas-Mélia, D., Chauvin, F., Déqué, M., Douville, H., Guérémy, J.-F., Marquet, P., Planton, S., Royer, J.F., Tyteca, S., 2005. Description and validation of the CNRM-CM3 global coupled model. CNRM Work. Note 103, 36.
Sapart, C.J., Monteil, G., Prokopiou, M., van de Wal, R.S.W., Kaplan, J.O., Sperlich, P., Krumhardt, K.M., van der Veen, C., Houweling, S., Krol, M.C., Blunier, T., Sowers, T., Martinerie, P., Witrant, E., Dahl-Jensen, D., Röckmann, T., 2012. Natural and anthropogenic variations in methane sources during the past two millennia. Nature 490, 85–88. http://dx.doi.org/10.1038/nature11461.
Schaefer, H., Whiticar, M.J., Brook, E.J., Petrenko, V.V., Ferretti, D.F., Severinghaus, J.P., 2006. Ice record of $\delta^{13}C$ for atmospheric CH_4 across the Younger Dryas-Preboreal transition. Science 313, 1109–1112. http://dx.doi.org/10.1126/science.1126562.
Schmidt, G.A., Ruedy, R., Hansen, J.E., Aleinov, I., Bell, N., Bauer, M., Bauer, S., Cairns, B., Canuto, V., Cheng, Y., Del Genio, A., Faluvegi, G., Friend, A.D., Hall, T.M., Hu, Y., Kelley, M., Kiang, N.Y., Koch, D., Lacis, A.A., Lerner, J., Lo, K.K., Miller, R.L., Nazarenko, L., Oinas, V., Perlwitz, J., Perlwitz, J., Rind, D., Romanou, A., Russell, G.L., Sato, M., Shindell, D.T., Stone, P.H., Sun, S., Tausnev, N., Thresher, D., Yao, M.-S., 2006. Present-day atmospheric simulations using GISS ModelE: comparison to in situ, satellite, and reanalysis data. J. Clim. 19, 153–192. http://dx.doi.org/10.1175/JCLI3612.1.
Schuldt, R.J., Brovkin, V., Kleinen, T., Winderlich, J., 2013. Modelling Holocene carbon accumulation and methane emissions of boreal wetlands – an Earth system model approach. Biogeosciences 10, 1659–1674. http://dx.doi.org/10.5194/bg-10-1659-2013.
Schumann, U., Huntrieser, H., 2007. The global lightning-induced nitrogen oxides source. Atmos. Chem. Phys. 7, 3823–3907. http://dx.doi.org/10.5194/acp-7-3823-2007.
Singarayer, J.S., Valdes, P.J., Friedlingstein, P., Nelson, S., Beerling, D.J., 2011. Late Holocene methane rise caused by orbitally controlled increase in tropical sources. Nature 470, 82–85. http://dx.doi.org/10.1038/nature09739.
Sowers, T., 2006. Late Quaternary atmospheric CH_4 isotope record suggests marine clathrates are stable. Science 311, 838–840. http://dx.doi.org/10.1126/science.1121235.
Spahni, R., Chappellaz, J., Stocker, T.F., Loulergue, L., Hausammann, G., Kawamura, K., Flückiger, J., Schwander, J., Raynaud, D., Masson-Delmotte, V., Jouzel, J., 2005. Atmospheric methane and nitrous oxide of the Late Pleistocene from Antarctic Ice Cores. Science 310, 1317–1321. http://dx.doi.org/10.1126/science.1120132.
Stauffer, B., Lochbronner, E., Oeschger, H., Schwander, J., 1988. Methane concentration in the glacial atmosphere was only half that of the preindustrial Holocene. Nature 332, 812–814. http://dx.doi.org/10.1038/332812a0.
Stevenson, D.S., Dentener, F.J., Schultz, M.G., Ellingsen, K., van Noije, T.P.C., Wild, O., Zeng, G., Amann, M., Atherton, C.S., Bell, N., Bergmann, D.J., Bey, I., Butler, T., Cofala, J., Collins, W.J., Derwent, R.G., Doherty, R.M., Drevet, J., Eskes, H.J., Fiore, A.M., Gauss, M., Hauglustaine, D.A., Horowitz, L.W., Isaksen, I.S.A., Krol, M.C., Lamarque, J.-F., Lawrence, M.G., Montanaro, V., Müller, J.-F., Pitari, G., Prather, M.J., Pyle, J.A., Rast, S., Rodriguez, J.M., Sanderson, M.G., Savage, N.H., Shindell, D.T., Strahan, S.E., Sudo, K., Szopa, S., 2006. Multimodel ensemble simulations of present-day and near-future tropospheric ozone. J. Geophys. Res. Atmos. 111, D08301. http://dx.doi.org/10.1029/2005JD006338.
Stone, E.J., Lunt, D.J., Annan, J.D., Hargreaves, J.C., 2013. Quantification of the Greenland ice sheet contribution to Last Interglacial sea level rise. Clim. Past 9, 621–639. http://dx.doi.org/10.5194/cp-9-621-2013.
Svendsen, J.I., Alexanderson, H., Astakhov, V.I., Demidov, I., Dowdeswell, J.A., Funder, S., Gataullin, V., Henriksen, M., Hjort, C., Houmark-Nielsen, M., Hubberten, H.W., Ingólfsson, Ó., Jakobsson, M., Kjær, K.H., Larsen, E., Lokrantz, H., Lunkka, J.P., Lyså, A., Mangerud, J., Matiouchkov, A., Murray, A., Möller, P., Niessen, F., Nikolskaya, O., Polyak, L., Saarnisto, M., Siegert, C., Siegert, M.J., Spielhagen, R.F., Stein, R., 2004. Late Quaternary ice sheet history of northern Eurasia. Quat. Sci. Rev. Quat. Environ. Eurasian North (QUEEN) 23, 1229–1271. http://dx.doi.org/10.1016/j.quascirev.2003.12.008.
Tarasov, P., Granoszewski, W., Bezrukova, E., Brewer, S., Nita, M., Abzaeva, A., Oberhänsli, H., 2005. Quantitative reconstruction of the last interglacial vegetation and climate based on the pollen record from Lake Baikal, Russia. Clim. Dyn. 25, 625–637. http://dx.doi.org/10.1007/s00382-005-0045-0.
Telford, P.J., Abraham, N.L., Archibald, A.T., Braesicke, P., Dalvi, M., Morgenstern, O., O'Connor, F.M., Richards, N.A.D., Pyle, J.A., 2013. Implementation of the Fast-JX Photolysis scheme (v6.4) into the UKCA component of the MetUM chemistry-climate model (v7.3). Geosci. Model Dev. 6, 161–177. http://dx.doi.org/10.5194/gmd-6-161-2013.
Thompson, A.M., Chappellaz, J.A., Fung, I.Y., Kucsera, T.L., 1993. The atmospheric CH_4 increase since the Last Glacial Maximum. Tellus B 45, 242–257. http://dx.doi.org/10.1034/j.1600-0889.1993.t01-2-00003.x.
Turetsky, M.R., Kotowska, A., Bubier, J., Dise, N.B., Crill, P., Hornibrook, E.R.C., Minkkinen, K., Moore, T.R., Myers-Smith, I.H., Nykänen, H., Olefeldt, D., Rinne, J., Saarnio, S., Shurpali, N., Tuittila, E.-S., Waddington, J.M., White, J.R., Wickland, K.P., Wilmking, M., 2014. A synthesis of methane emissions from 71 northern, temperate, and subtropical wetlands. Glob. Change Biol. 20, 2183–2197. http://dx.doi.org/10.1111/gcb.12580.
Turney, C.S.M., Jones, R.T., 2010. Does the Agulhas Current amplify global temperatures during super-interglacials? J. Quat. Sci. 25, 839–843. http://dx.doi.org/10.1002/jqs.1423.
Valdes, P.J., Beerling, D.J., Johnson, C.E., 2005. The ice age methane budget. Geophys. Res. Lett. 32 http://dx.doi.org/10.1029/2004GL021004.
Valentin, K.M., 1990. Numerical Modeling of the Climatological and Anthropogenic Influences on the Chemical Composition of the Troposphere since the Last Glacial Maximum. Mainz.
Velichko, A.A., Novenko, E.Y., Pisareva, V.V., Zelikson, E.M., Boettger, T., Junge, F.W., 2005. Vegetation and climate changes during the Eemian interglacial in Central and Eastern Europe: comparative analysis of pollen data. Boreas 34, 207–219. http://dx.doi.org/10.1111/j.1502-3885.2005.tb01016.x.
Voulgarakis, A., Naik, V., Lamarque, J.-F., Shindell, D.T., Young, P.J., Prather, M.J., Wild, O., Field, R.D., Bergmann, D., Cameron-Smith, P., Cionni, I., Collins, W.J., Dalsøren, S.B., Doherty, R.M., Eyring, V., Faluvegi, G., Folberth, G.A., Horowitz, L.W., Josse, B., MacKenzie, I.A., Nagashima, T., Plummer, D.A., Righi, M., Rumbold, S.T., Stevenson, D.S., Strode, S.A., Sudo, K., Szopa, S., Zeng, G., 2013. Analysis of present day and future OH and methane lifetime in the ACCMIP simulations. Atmos. Chem. Phys. 13, 2563–2587. http://dx.doi.org/10.5194/acp-13-2563-2013.
Wahlen, M., Tanaka, N., Henry, R., Deck, B., Zeglen, J., Vogel, J.S., Southon, J., Shemesh, A., Fairbanks, R., Broecker, W., 1989. Carbon-14 in methane sources and in atmospheric methane: the contribution from Fossil carbon. Science 245, 286–290. http://dx.doi.org/10.1126/science.245.4915.286.
Weber, S.L., Drury, A.J., Toonen, W.H.J., van Weele, M., 2010. Wetland methane emissions during the Last Glacial Maximum estimated from PMIP2 simulations: climate, vegetation, and geographic controls. J. Geophys. Res. Atmos. 115 http://dx.doi.org/10.1029/2009JD012110.
Whiticar, M., Schaefer, H., 2007. Constraining past global tropospheric methane budgets with carbon and hydrogen isotope ratios in ice. Philos. Trans. R. Soc. Math. Phys. Eng. Sci. 365, 1793–1828. http://dx.doi.org/10.1098/rsta.2007.2048.
Wolff, E., Spahni, R., 2007. Methane and nitrous oxide in the ice core record. Philos. Trans. R. Soc. Math. Phys. Eng. Sci. 365, 1775–1792. http://dx.doi.org/10.1098/rsta.2007.2044.
Yvon-Durocher, G., Allen, A.P., Bastviken, D., Conrad, R., Gudasz, C., St-Pierre, A., Thanh-Duc, N., del Giorgio, P.A., 2014. Methane fluxes show consistent temperature dependence across microbial to ecosystem scales. Nature 507, 488–491. http://dx.doi.org/10.1038/nature13164.
Zhou, B., Shen, C., Sun, W., Zheng, H., Yang, Y., Sun, Y., An, Z., 2007. Elemental carbon record of paleofire history on the Chinese Loess Plateau during the last 420 ka and its response to environmental and climate changes. Palaeogeogr. Palaeoclimatol. Palaeoecol. 252, 617–625. http://dx.doi.org/10.1016/j.palaeo.2007.05.014.
Zhou, X., 2012. Asian monsoon precipitation changes and the Holocene methane anomaly. Holocene 22, 731–738. http://dx.doi.org/10.1177/0959683611430408.
Zürcher, S., Spahni, R., Joos, F., Steinacher, M., Fischer, H., 2013. Impact of an abrupt cooling event on interglacial methane emissions in northern peatlands. Biogeosciences 10, 1963–1981. http://dx.doi.org/10.5194/bg-10-1963-2013.